CP No 152
(14,672)
A.R C. Technical Report

MINISTRY OF SUPPLY

AERONAUTICAL RESEARCH COUNCIL

CURRENT PAPERS

Stationary Rig Experiments on the Heat Extracting Power of Closed Thermosyphon Cooling Holes

By

Dr. H. W. Hahnemann

LONDON HER MAJESTY'S STATIONERY OFFICE

1954

Price 3s 6d net

Current Paper No. 152

Corrigenda

November, 1951

Page 8, penultimate line, page 9, equation (25), and figure 16, in the portion of the equation:-

$$\frac{\left(0.1392 \frac{L}{di}\right)^{1.85}}{\left(0.415 \frac{L'}{di}\right)^{21}}$$

quoted, the indices are incorrectly written, and the whole equation should read:-

$$j = \frac{Nu}{Pr2/3} \frac{\left(0.1392 \frac{L}{di}\right)^{1.835} (1 - 0.0979\ Pr^{0.4035})}{\left(0.415 \frac{L'}{di}\right)^{0.21} (1.05\ Pr^{0.01} - 1)}$$

Page 15, equation (10), ρs has been omitted from the right-hand side of the equation, and should read:-

$$\sigma = \rho s \int_{P_o}^{P_2} \frac{dP}{\rho}$$

Page 17, line 2, "thermocyphon" should read "thermosyphon".

Page 18, line 11, "calculatins" should read "calculations".

Page 20, line 3, "respevtively" should read respectively".

C.P. No. 152

Memorandum No. M.128.

November, 1951.

NATIONAL GAS TURBINE ESTABLISHMENT

Stationary Rig Experiments on the Heat Extracting Power of Closed Thermosyphon Cooling Holes

- by -

Dr. H.W. Hahnemann

SUMMARY

In order to fill a gap in our knowledge of blade cooling methods, some stationary rig experiments have been made on heat flow in closed thermosyphon holes, with the object of providing information on heat flow in closed sodium-filled holes in turbine blades. The stationary rig was simply a tube filled with fluid, transferring heat upwards by free convection from an electrically heated lower section to a water cooled upper section. The high Grashof numbers obtained in closed thermosyphon holes in actual turbine blades were approached by using large tube diameters, and to cover a wide range of Grashof numbers and Prandtl numbers, measurements were made with mercury, water and oil as the heat transporting fluid. A formula correlating the results for the three different fluids was obtained. These results can be extended to the case of sodium, and heat transfer curves for various hole diameters, lengths and accelerations can be constructed (e.g. Figure 18). No measurements beyond the boiling point of the fluids were attempted, and the closely connected problem of what form of cooling can be applied to the blade roots is not dealt with. The relationship of the "closed" thermosyphon method to the "open" or Schmidt thermosyphon method is briefly discussed.

CONTENTS

APPENDICES

ILLUSTRATIONS AND TABLES

ILLUSTRATIONS AND TABLES (cont'd)

1.0 Introduction

For the complete calculation of internal turbine blade cooling a series of heat resistances must be known, i.e.

(a) The external heat resistance between the hot working gas in the turbine and the blade surface, which has up to now been investigated more than the other relevant heat resistances, and which has been summarized for instance by A.G. Smith [1,2]* or T.W.F. Brown [3]. This resistance will not be dealt with in the subsequent report.

(b) Resistances due to heat conduction in the solid blade material, also not considered here, may be best obtained experimentally or by relaxation methods. Only in a few cases is an exact calculation rendered possible by highly idealised boundary conditions (A.G. Smith [2]).

(c) Heat resistance between blade and coolant inside the blade about which there is little known except for the case where pressure air is injected into the hot gas stream by straight tubular passages leading from the root of the blade to the tip and discharging there. The cooling efficiency of air in this arrangement, however, is not high unless a fairly complicated internal structure is used. Forced convection of water offers the possibility of easier internal cooling.

A variety of other methods for internal cooling has been proposed in literature. Among these sweat cooling (also called injection cooling or effusion cooling) and thermosyphon cooling show very promising features. In effusion cooling by means of porous blade material it can be safely assumed that the coolant reaches the blade surface temperature. The pressure drop required to force the coolant through the blade can be approximately calculated from data given for instance by P. Grootenhuis [4], while the reduction of the outer heat transfer coefficient by the influence of homogeneous injection into the laminar gas-side boundary layer has been estimated theoretically by R. Staniforth [5].

The thermosyphon method for internal blade cooling can be applied either in the open or in the closed form of the circulating system. In the open system, first applied to turbine blades by Holzwarth [6] and sometimes called the Schmidt cooling, straight passages in the blade, closed at the blade tip are fed with water from the hollow hub by the action of centrifugal forces alone and the generated steam is extracted through the hollow hub for condensation preferably in connection with some other useful purpose. As is shown in Appendix I under the assumption that open thermosyphon cooling at high acceleration forces is extremely powerful, especially if the water reaches the critical state in the cooling passages, (heat transfer coefficients of the order 1600 to 6000 Chu./sq.ft. hr.°C or 0.44 to 1.70 Chu./sq.ft.sec.°C being expected), the open system may in some cases provide too much heat extraction.

It seems therefore worthwhile to consider the closed thermosyphon system as an alternative. In this closed system the cooling passages are closed at both ends as is schematically shown in Figure 3 and a separate cooling system is arranged at the blade roots through the hollow hub. If the thermosyphon liquid were able to confer on the blade an apparent thermal conductivity equal to that of solid copper, the necessary amount of heat for cooling could be extracted from the blade root. The additional heat resistance between root and root coolant produces a higher working temperature of the thermosyphon liquid as

---

* The figures in squared brackets relate to the list of references at the end of report.

compared with the open system and, therefore, instead of water other fluids must be employed which at the limiting centrifugal pressure of about 3200 lb./sq.in. and at temperatures higher than t_c = 375°C are still below the critical and are therefore of high density. This requirement is automatically satisfied by liquid metals and it has been the major object of this report to determine the heat extracting power of liquid metals in closed thermosyphon holes.

The question arises whether the radial pressure distribution due to centrifugal forces and its relation to the stress exerted on the blade by the same centrifugal forces is more favourable in either the open or the closed thermosyphon system. An approach to answer this question has been attempted in Appendix II.

From the considerations in Appendix II it also follows that liquid sodium may be a convenient means for closed thermosyphon cooling. For a simple investigation of this problem a stationary rig was chosen having relatively large dimensions. Since the handling and heating up of sodium in large quantities is dangerous in the absence of special precautions, mercury was used instead. The results must then be transferred to sodium theoretically and the method of doing so is outlined in Appendix III. In order to provide the necessary information for this transformation, similar tests were carried out with water and transformer oil as well.

Previous attempts to obtain information on thermosyphon cooling have been mainly concerned with socalled "harps" where a closed loop of pipe is heated at the lower end of one vertical leg and cooled at the upper end of the other. References on this subject are, for instance, given in liquid-metals handbook [7]. Other arrangements were designed with respect to open thermosyphon cooling of turbine blades and permit no direct application to closed systems.

2.0 Test rig assembly and test procedure

The main features of the test elements are shown schematically in Figure 4 and the geometrical dimensions of the different elements are given in Table 1.

The heated part of length L of the test element contained along a generating line on the outer surface a number of chromel-alumel thermocouples (indicating temperatures t_0, t_1, t_2, ... along the wall) which were inserted into small holes and silver soldered to the surface. Another couple measured the temperature ϑ on the same generating line at a position in the middle of the cooling coil. The heated surface was covered with two layers of thin asbestos sheet put on wet and dried out afterwards. Round the asbestos the 21 S.W.G. constantan heating wire was wound tightly and held in position by further layers of asbestos ribbon so that the leads to the heating coil entered at the lower end and the leads to the thermocouple junctions entered normal to the wall between the heating coil. For this purpose spaces were left between the turns of the coil and the leads protected by embedding them into cones of castable cement.

The test element was then inserted with its lower end up to the cooling block into a large container filled with kieselguhr for heat insulation and was held vertically by means of tripods and clamps. The thermosyphon liquid, being mercury, water or transformer oil, was filled to the level of the upper end of the cooling block. A thermometer in the tube centre indicated the temperature in the axis at the same position as the thermocouple for measuring ϑ. Four arrangements were tested. "a" had an external cooling coil with counterflow, "b" an external cooling coil with parallel flow, "c" an internal cooling coil, and "d" both internal and external cooling coils. The arrangements are described in more detail in the footnote to Table 1. In the case of cooling arrangements "c" and "d", this thermometer was replaced by a sealed thermocouple. Another thermocouple sealed in a long tube of quartz glass was used to probe around in the thermosyphon liquid to obtain some information on the temperature distribution and the movement of the liquid.

Inlet and outlet temperatures θ_o and θ_1 of the cooling water, from which the arithmetic mean $\theta_m = (\theta_o + \theta_1)/2$ was formed, were measured by thermometers embedded in thermometer pockets. The cooling water was taken from a constant level tank in order to reduce fluctuations in flow rate and inlet temperature from the water main. The coolant flow rate was measured by weighing quantities of water M leaving the cooling coil and measuring the discharge time z by means of a 1/5 sec. stop watch. This was done several times during each test with a specified heat input and the heat extraction q was calculated with averaged values from the formula.

$$q = \frac{M}{z} C_{p_w} (\theta_1 - \theta_o) \qquad \ldots \quad \ldots \quad \ldots \quad \ldots \quad \ldots \quad (22)$$

with C_{p_w} = specific heat of the water. Applying equation (16) from Appendix III the Nusselt number then follows from

$$Nu = \frac{h\, d_i}{\lambda} = \frac{M\, C_{p_w} (\theta_1 - \theta_o)}{\pi\, z\, L\, \lambda (t_o - \theta_m)} . \qquad \ldots \quad \ldots \quad \ldots \quad (23)$$

The heat input was taken from the 230 volts a.c. main and was regulated in arbitrary steps by means of a Variac transformer. An estimate of the heat generation by eddy currents in a mercury column in the centre of a coil shows that this possible source of error can be neglected. Heat losses to the ambient air were reduced as much as possible by surrounding all parts concerned with crushed aluminium foil. In some cases the electrical input was measured and compared with q calculated from equation (22). The difference was in all cases small and was in accordance with theoretical calculations of the heat losses by free convection in still air.

The thermocouple leads were all connected to a selector switch and all the temperature readings by means of thermocouples were taken against an ice junction using a quick reading potentiometer. The accuracy was of no great importance since, especially in the case of mercury and for not too small temperature differences $\Delta T = t_o - \theta_m$, large fluctuations occurred indicating that the liquid did not circulate in a quasi-steady swirl but rather in irregular masses.

In order to find whether the wetting effect of mercury is important, some tests were carried out with induced wetting. The method of dissolving magnesium in mercury proved unsatisfactory as after a short while, though wetting was favoured, the magnesium oxide produced formed patches of scum. A mild steel tube was therefore covered inside with Tinmans solder in one case, and in another case was copper plated and brazed afterwards. From the appearance of the mercury miniscus wetting seemed to have occurred, but no appreciable rise in heat extraction was measured. One of the test elements was made of solid copper in order to permit a comparison based on apparent thermal conductivities. As is shown in Table 1 each test element and each filling and cooling arrangement has been given a certain symbol which is kept in all the consecutive plots in order to save lengthy explanations for each of them.

3.0 Evaluation of the results

For all cases the temperature t_o nearest to the hot end of the vertical tube, t_o being chosen as one of the standard temperatures, was measured between $\frac{1}{4}$ and $\frac{1}{2}$" away from the bottom surface. Some typical measured temperature distributions are shown in Figures 5 to 8. They are results from test elements filled with mercury, water and transformer oil respectively while Figure 8 is for the solid copper bar. Each test series took about two days including the waiting times to reach steady state after having altered the heat input but not all the curves are plotted for the elements under consideration. The large fluctuations in the case of mercury fillings are represented in Figure 5 by plotting the extreme temperature indication on either side of each curve. These fluctuations indicate that a steady double vortex is not formed in the

tube but rather that unsteady large masses of liquid move at random. By putting a dust layer on the mercury surface these masses could be clearly observed when they rose to the surface, and a definite correlation was found between the temperature fluctuations and the movement of these masses of liquid.

The parameter on the curves is the total heat input q. As the diagrams show, quite different shapes of the temperature distributions are possible ranging from almost parabolic shapes near the hot end in the case of the solid copper bar to shapes with maximum temperature situated somewhere between the ends of tube as in the case of transformer oil fillings. According to formula (1), Appendix I, the temperature drop across the tube wall is only of the order 0.5 deg. C, and therefore these temperature distributions can be considered to represent the distribution along the inner wall as well.

Applying equation (20), Appendix III, and $\lambda_{M_{Cu}} = 0.0051$ Chu./in. sec. °C theoretical distributions result for the solid copper bar which in some cases ($t_o = 386$°C and $q = 0.566$ Chu./sec., $t_o = 322$°C and $q = 0.456$ Chu./sec., $t_o = 238$°C and $q = 0.342$ Chu./sec., $t_o = 102$°C and $q = 0.132$ Chu./sec.) are plotted in Fig. 8 as dashed curves. A comparison of these dashed curves with the measured distributions shows, that especially for not too small $t_o - \vartheta$ and near the hot end the heat input per unit length is almost independent of distance x from lower end, thus justifying the applicability of equation (20).

Applying equation (20), though it is not quite justified, also for the thermosyphon tubes, the ratio of apparent conductivity λapp to the conductivity of copper $\lambda_{M_{Cu}}$ (see Appendix II) is approximately given by

$$\frac{\lambda app}{\lambda_{M_{Cu}}} = \frac{q\,x^2}{0.0102\,AL(t_o - t)} \quad \ldots \quad \ldots \quad \ldots \quad \ldots \quad (24)$$

When we choose $x = 0.75L$ and the corresponding t from the curves, in order to eliminate the effect of the cooled end, equation (24) becomes

$$\frac{\lambda app}{\lambda_{M_{Cu}}} = 55\,2\,\frac{qL}{A(t_o - t_{x = 0.75L})} \quad \ldots \quad \ldots \quad (24a)$$

Some of these ratios, calculated from equation (24a) by means of the measured heat inputs q and temperature distributions are plotted in Fig. 9, but only for mercury and water fillings. For some examples $\lambda_{app}/\lambda_{M_{Cu}}$ ratios were read off Fig. 9 and with these, temperature distributions were calculated with equation (20) and the results plotted as dashed lines in Figs. 5 and 6. For water the agreement with the measured distributions is quite reasonable but not so good for mercury.

Figs. 10a and 10b contain the measured heat extractions q versus $\Delta T = t_o - \vartheta_m$, t_o being the outer wall temperature as measured nearest to the lower end of the tube and ϑ_m being the mean temperature of the cooling water. The reasons why this ΔT has been chosen for correlations is explained in Appendix III. In order to avoid confusion only results with cooling arrangements "a" and "b" are plotted in Figs. 10a and 10b this also being the reason for plotting them on two different sheets. The direction of flow of the cooling water, which is the only difference between methods "a" and "b", had no influence on the results. In Fig. 10c the results obtained with cooling arrangements "c" and "d" are plotted in the same manner together with the results for tube 10 with cooling arrangement "a". This tube 10 behaves differently compared with the others probably due to the copper plating and the large cooled length L'.

These different cooling arrangements were investigated for reasons as follows. The cooling efficiency would probably be greatest if the liquid moved steadily in the direction of gravity down the centre of the tube and

rose against this direction along the tube walls by being heated up there and driven upwards by the density difference between wall and centre fluid. The simplest cooling arrangement "a" with cooling coil round the outer upper part of the tube however creates a large total vertical density difference adjacent to the wall. The cooled fluid directly adjacent to the cooling coil therefore sinks down at the wall and thus upsets the natural thermosyphon swirl. This may be the reason why large L/d_i ratios are rather ineffective. The natural vortex swirl would be maintained better if the cooling coil could be arranged in the centre of the tube instead of round the outer wall of the tube. Cooling arrangement "c" consists of such an "inner" coil in the centre of the hole, and in favourable cases the heat extraction at the same ΔT was about 40% higher than with cooling arrangement "a". Unfortunately this inner coil had to be made of rather thick-walled small-bore steel tube so that its heat resistance was probably considerably higher than that of the outer copper tin-soldered coil thus reducing the favourable action especially in the case of high Prandtl number thermosyphon liquids. Cooling arrangement "d" which was a combination of "a" and "c", had therefore no advantage against "c" with a mercury filling (see the two upper curves in Fig. 10c) but was however better with the oil filling.

Another possibility of inducing more regular flow over the whole tube length L is the provision of an insert. In tube 2 of $d_i = 1.811$ in. a thin-walled tube of length 14 in. and outer dia. 1 in. was inserted so that its lower open end was at a distance of 1 in. from the bottom of the test tube and its upper open end roughly coincided with the centre of the cooling coil. Results with this insert together with cooling arrangement "a" were roughly equivalent to the results without insert and with arrangement "d".

For the final correlation of the results by means of the dimensionless groups as outlined in Appendix III only the results with cooling arrangements "a" and "b" as the most practical ones were employed. For forced or natural flows which are not connected with a swirl-like motion the parameter $Nu/Pr^{\frac{1}{3}}$ has been proved to be most useful. Attempts to apply this parameter over the vast range of Prandtl numbers investigated here failed. It was therefore decided after several other trials to apply $Nu/Pr^{2/3}$. This parameter is plotted versus Grashof number in Fig. 11. The properties as used for the calculations are shown in Figs. 12 to 14, and the properties for sodium (as used to transfer the results to sodium filled turbine blades) in Fig. 15. All the properties have to be taken at the temperature t_o of the hot end of the thermosyphon tube.

The remaining scatter in Fig. 11 is mainly attributed to the L/d_i ratio and to lesser degrees to the cooling length ratio L'/d_i, temperature ratio, and to heat resistances of the heat input and cooling systems. A correlation of the heat resistances had to remain unconsidered. The temperature ratio taken for hot and cold end would leave the low Grashof number points unaltered for each test series. Only the higher Gr points in Fig. 11 could be moved and the scatter would remain. It was therefore considered that the Prandtl number in connection with ΔT in Gr and Nu provides sufficient correlation for the temperature ratio. Next the correlation for the heating length diameter ratio L/d_i was attempted. It was not possible to choose a universal constant for the power m_3 in $(L/d_i)^{m3}$ of equation (17), Appendix III. A reasonable power m_3 found after several trials left some of the curves still poorly fitted into the general trend. These were improved by a further cooling length diameter ratio correction. The final choice then was

$$\frac{Nu}{Pr^{2/3}} \; \frac{\left(0.1392 \; \frac{L}{d_i}\right)^{1.85} \left(1 - 0.0979 \; Pr^{0.4035}\right)}{\left(0.415 \; \frac{L'}{d_i}\right)^{.21} \left(1.05 \; Pr^{0.01} - 1\right)} = j$$

which should be a function of Grashof number alone.

This parameter j is plotted against Gr in Fig. 16. For each test tube with the exceptions of tube 10 (as mentioned above) and tube 7 with oil filling a curve results which at the higher range of its Gr fits satisfactory to a straight line represented by

$$j = \frac{Nu}{Pr^{2/3}} \frac{\left(0.1392 \frac{L}{d_i}\right)^{1.85} \left(1 - 0.0979\ Pr^{0.4035}\right)}{\left(0.415 \frac{L'}{d_i}\right) 21 \left(1.05\ Pr^{0.01} - 1\right)} = 0.002837\ Gr^{0.372} \quad \ldots (25)$$

Towards lower Grashof numbers the individual test curves leave this general straight line, becoming less steep in a certain transition range and finally, at small Gr, i.e. at very small ΔT, all the curves turn into the horizontal, where obviously laminar flow conditions prevail.

According to these results equation (25) should provide satisfactory means for the computation of heat extractions by closed thermosyphon tubes for all cases where:

(a) no changes of state are concerned,
(b) the temperature difference ΔT between hot end and cold end is not too small,
(c) the heat resistance of the heat extraction system is not too high.

If condition (c) is not satisfied this heat resistance may be taken into account separately, i.e. additionally.

4.0 Application to turbine cooling

For sodium as the probable means for closed thermosyphon cooling in turbines the temperature in the holes will be of the order 250 to 600 deg. C and therefore the Prandtl number of the order 0.006 to 0.002. For the small Pr numbers the L'/d_i correction is practically negligible and also the power of the L/d_i term is practically constant. Equation (25) then simply turns into

$$j = \frac{Nu}{Pr^{2/3}} \left(0.1392 \frac{L}{d_i}\right)^{1.835} = 0.002837\ Gr^{0.372} \quad \ldots \quad \ldots \quad \ldots \quad (26)$$

This is a very simple and convenient working formula for liquid sodium and is plotted in Fig. 17 as $Nu/Pr^{2/3}$ vs. L/d_i with Gr as parameter.

Assuming now as practical figures for an example: acceleration due to centrifugal forces b = 20 000 g, where g = 32 ft./sec^2.; $d_i = \frac{1}{8}$ inch; ΔT = 300 deg.C with hot end temperature t_o = 600 deg. C and where from Fig. 15 Pr = 0.0023, ν = 0.0061 ft^2./hr., λ = 34.5 Chu./ft.hr.°C, β = 0.000271 per deg. C, the Grashof number is calculated as Gr = 2.05 x 10^{10}, and herewith form equation (26)

$$Nu/Pr^{2/3} = 19.4 / (0.1392\ L/d_i)^{1.835} \quad \text{(dashed line in Fig. 17).}$$

Combining this equation with equation (16), Appendix III, and inserting the value for $Pr^{2/3}$ leads to

$$q = \frac{0.338\ \pi\ L\ \Delta T \lambda}{\left(0.1392\ L/d_i\right)^{1.835}}$$

for the heat extraction q, or for the assumed figures

$$q = 3.06 \frac{L}{\left(0.1392\ L/d_i\right)^{1.835}} \text{ Chu./sec., with L and } d_i \text{ in feet.} \quad \ldots (27)$$

If under the same conditions as above $d_1 = 1/6$ inch is possible instead of $d_i = 1/8$ inch due to a thicker blade the corresponding formulae are easily derived as

$$Gr = 4.85 \times 10^{10},\ Nu/Pr^{2/3} = 26.9 \Big/ \left(0.1392\ \frac{L}{d_1}\right)^{1.835} \text{ and}$$

$$q = 4.24\ \frac{L}{\left(0.1392\ L/d_i\right)^{1.835}} \quad \ldots \quad \ldots \quad \ldots \quad (27a)$$

These conditions are plotted in Fig. 18 from which it can at once be seen whether a desired q can be extracted by the thermosyphon effect for a given blade permitting a hole of length L and diameter d_1.

If, for instance, for a certain turbine layout, the blades can be provided with 5 holes and the heat extraction must be 1.5 Chu./sec. per blade in order to keep the blade surface at a sufficiently low temperature the necessary heat per hole q = 0.3 Chu./sec. cannot be extracted with L/d_1 ratios larger than 5.2 or 10.8 or 17.5 respectively if the blade thickness does not allow for bores of d_i larger than 1/8 or 1/6 or 1/5 inch.

With the data given here it is easy to establish diagrams in the manner of Fig. 18 for any other general conditions.

5.0 Conclusions

The heat extracting power of the blind thermosyphon system has been investigated experimentally covering a range of Prandtl numbers from 0.005 to 400, of Grashof numbers from 10^4 to 10^{10} and of length diameter ratio from 3.5 to 14. In spite of these wide variations the results could be correlated satisfactorily be a proper dimensionless grouping and thus closely approximated by a mathematical formula. This formula becomes very simple for liquid metals as a potential means for turbine blade cooling and the development of diagrams is laid out from which it can at once be seen which blade size is able to extract a given quantity of heat. The total heat flow through the blade from working gas to cooling air in the hollow hub via thermosyphon system has to be calculated by a step by step procedure, by taking into account the heat resistances between gas and blade surface, outer and inner blade surface, and root and cooling air.

REFERENCES

No.	Author	Title
1	A.G. Smith	Heat Flow in the Gas Turbine. Proc. Inst. Mech. Engrs., vol. 159 (1948) W.E.I. No. 41, p.245.
2	A.G. Smith and R.D. Pearson	The Cooled Gas Turbine. Proc. Inst. Mech. Engrs., vol. 163 (1950) W.E.P. No. 60, p.221.
3	T.W.F. Brown	Some factors in the use of high temperatures in Gas Turbines. Proc. Inst. Mech. Engrs., vol. 162 (1950), p.167.
4	P. Grootenhuis	The flow of gases through porous metal compacts. Engng., vol. 167 (1949), No.4340, p.291.
5	R. Staniforth	Contribution to the theory of effusion cooling of gas-turbine blades. Inst. Mech. Engrs. General Discussion on Heat Transfer. 11/13 Sept. 1951.

REFERENCES (Cont'd)

No.	Author	Title
6	H. Holzwarth	Die Entwicklung der Holzwarth-Gasturbine, Holzwarth-Gasturbinen GmbH, Muehlheim-Ruhr 1938.
7	R.N. Lyon and others	Liquid-metals handbook. Navexos P-733, 1.6.1950. Atomic Energy Comm. Washington.
8	E. Schmidt	Thermodynamics, principles and applications to Engineering, Oxford Univ. Press 1949.

APPENDIX I

The possible over-cooling effect of the open thermosyphon system

Supposing the temperature t_g of the driving gas in the first rotor stage is suitably so high that the heat flow of the open thermosyphon system just maintains a temperature t_{b_o} of the gas-side blade surface in accordance with the allowable stress under working conditions. In the following estimate, therefore, t_{b_o} is fixed as optimum and the magnitude of t_g, being of no immediate interest in this, would follow from proper consideration of the heat resistance concerned.

It can be shown that for at present known heat resistant blade materials their stress limit is just approached by speeds of the rotor which at the same time produce critical pressure in the water filling the inner passages. With $t_c^{\ast}$ as critical value of the coolant temperature t_c we may therefore assume that $(t_{b_o} - t_c^{\ast})$ over the wall thickness δ is from stress considerations the most favourable temperature drop for the heat flow (t_{b_o} being chosen, $t_c^{\ast}$ being forced upon us as we assume the water is saturated everywhere in the passages) and that t_g is adapted by the heat resistance between driving gas and blade surface.

Idealising the problem as shown in Fig. 1 by an infinitely extended cylindral rod with outside diameter d_o and with a straight hole of diameter d_i and which is heated by a gas stream from outside under constant temperature conditions over the outer and inner surfaces respectively, the amount Q of heat conducted across the wall of length L and of heat conductivity λ_M may be estimated from

$$Q = \frac{2\,\pi\, L\lambda_M (t_{b_o} - t_c^{\ast})}{\log_e (d_o/d_i)} = \frac{2.729\, L\lambda_M (t_{b_o} - t_c^{\ast})}{\log_{10} (d_o/d_i)} \quad \ldots \quad \ldots \quad (1)$$

With L = 1.0 in., t_{b_o} = 800°C, λ_M = 0.0025 Chu./ft. sec. °C as convenient figures for conventional gas turbine blades and $t_c^{\ast}$ = 375°C for water equation (1) reduces to

$$\log_{10} (d_o/d_i) = 0.242/Q \quad \ldots \quad \ldots \quad \ldots \quad (2)$$

with Q in Chu./sec. as heat extraction per hole of each blade.

A turbine with mass flow rate G of driving gas of temperature t_g and specific heat C_{p_g} may have n rotor blades with z cooling holes each and the total heat extraction should not exceed p percent. The permitted heat extraction per hole is then

$$Q \leq G t_g C_{p_g} p/n\, z \quad \ldots \quad \ldots \quad \ldots \quad \ldots \quad (3)$$

and combination of equations (2) and (3) yields

$$\log_{10} (d_o/d_i) = 0.242\, nz/G t_g C_{p_g} p \quad \ldots \quad \ldots \quad \ldots \quad (4)$$

For the special figures n = 200, z = 5, t_g = 1000°C and C_{p_g} = 0.283 Chu./lb.°C this is

$$\log_{10} (d_o/d_i) \geq 0.855/Gp, \quad \ldots \quad \ldots \quad (4a)$$

with G in lb./sec.

This relation (4a) is plotted in Fig. 2 as required minimum diameter ratio d_o/d_1 of the holes versus mass flow G through the turbine and with percentage of heat extraction as a parameter.

In view of manufacturing difficulties and of possible occurrence of "slugging" in the holes they should presumably not be made under 0.1 inch. Thus, for practical blade thicknesses, the upper limit for d_o/d_1 is probably of the order 5. For this limit and with the above figures it would, therefore, not be possible to extract less than 2 or 3 or 4 or 5% of the total heat load of the turbine for a turbine with mass flow less than 61 or 41 or 31 or 24.5 lb./sec. respectively.

Of course, for other conditions these limits may vary widely and also in the given example the assumption of $t_g = 1000°C$ is only a rough guess. It is, however, doubtless true that for a given heat extraction p there is a critical size for each type of gas turbine under which open thermosyphon cooling is liable to overcool and thus to reduce the total efficiency below that of the uncooled turbine. It seems therefore doubtful whether this cooling method is applicable to turbines of small output.

APPENDIX II

Relation between stress and radial pressure rise

Using symbols as shown in Fig. 3 where the left part represents a blade with open thermosyphon system and the right part respectively one with a closed system, the radial pressure variation in the fluid filled bores is given by

$$dP/dr = \rho r\omega^2 - \rho g \cos\varphi \quad \ldots \quad \ldots \quad \ldots \quad (5)$$

and the centrifugal force acting on the blade by

$$m_s r_s \omega^2 + m_1 r_1 \omega^2 = \sigma A \quad \ldots \quad \ldots \quad \ldots \quad (6)$$

with:-

P = static pressure at radial distance r in the coolant which is in equilibrium with all the acting forces,

ρ = density of coolant,
ω = angular velocity,
g = acceleration due to gravity,
φ = angle between blade axis and direction of gravity,
m_s = mass of blade material,
m_1 = mass of coolant in holes,
r_s = radius of gyration for solid material,
r_1 = radius of gyration for liquid material,
A = total cross-section of solid material,
σ = stress exerted upon blade.

Neglecting the generally small gravity term in equation (5) we obtain for the open system

$$\int_{P_o}^{P_2} \frac{dP}{\rho_1} = \tfrac{1}{2}\omega^2(r_2^2 - r_1^2) \quad \ldots \quad \ldots \quad \ldots \quad (7a)$$

with r_2 and r_1 as outer and inner radii of the liquid column (of density ρ_1) where the pressures P_2 and P_o respectively may exist.

For the closed system an expansion cavity may be provided by means of which the same lower pressure P_o is maintained for all working conditions. Therefore, the inner radius may vary between r_3 in cold state and r_4 in hot state. This variation may be disregarded and the inner radius simply be taken as r_4 for all temperatures. We obtain then for the closed system

$$\int_{P_o}^{P_3} \frac{dP}{\rho_2} = \tfrac{1}{2}\omega^2(r_2^2 - r_4^2) \quad \ldots \quad \ldots \quad \ldots \quad (7b)$$

with P_3 and P_o as pressures at r_2 and r_4 respectively, and ρ_2 as density of the liquid.

In equation (6) it is $m_s = A(r_o - r_i)\rho_s$ and $r_s \approx \tfrac{1}{2}(r_o + r_i)$ for both open and closed systems and with ρ_s as density of blade material, and further for the open system $m_1 = (r_2 - r_1)\rho_{1_m} \Sigma f$, $r_1 \approx \tfrac{1}{2}(r_2 + r_1)$, and for the closed system $m_1 = (r_2 - r_4)\rho_{2_m} \Sigma f$, $r_1 = \tfrac{1}{2}(r_2 + r_4)$.

The different r symbols are explained in Fig. 3, suffix m relates to mean values of the densities, and Σf is the cross section for all the passages in the blade.

Consequently for the open system (suffix 1 at stress σ)

$$\sigma_1 = \tfrac{1}{2}\rho_s\omega^2\left[\left(r_o^2 - r_i^2\right) + \left(r_2^2 - r_1^2\right)\frac{\rho_{1m}}{\rho_s}\frac{\Sigma f}{A}\right] \ldots \quad (8a)$$

and for the closed system (suffix 2 at stress σ)

$$\sigma_2 = \tfrac{1}{2}\rho_s\omega^2\left[\left(r_o^2 - r_i^2\right) + \left(r_2^2 - r_4^2\right)\frac{\rho_{2m}}{\rho_s}\frac{\Sigma f}{A}\right] \ldots \quad (8b)$$

Only a slight error will be introduced into these equations when replacing r_o by r_2, and combining then equations (7a) with (8a) and (7b) with (8b) respectively gives for the open system

$$\sigma_1 = \rho_s\int_{P_o}^{P_2}\frac{dP}{\rho_1} - \tfrac{1}{2}\rho_s\omega^2\left[\left(r_i^2 - r_1^2\right) - \left(r_2^2 - r_1^2\right)\frac{\rho_{1m}}{\rho_s}\frac{\Sigma f}{A}\right] \ldots \quad (9a)$$

and for the closed system

$$\sigma_2 = \rho_s\int_{P_o}^{P_3}\frac{dP}{\rho_2} + \tfrac{1}{2}\rho_s\omega^2\left[\left(r_4^2 - r_i^2\right) + \left(r_2^2 - r_4^2\right)\frac{\rho_{2m}}{\rho_s}\frac{\Sigma f}{A}\right] \ldots \quad (9b)$$

For the same liquid and under the same general conditions σ_2 may be slightly higher than σ_1. For practical cases, the ratios ρ_m/ρ_s and $\Sigma f/A$ will be of the order 1/10 (for water) and 1/5 respectively, and inserting typical values for ρ_s, ω and the radii shows that the two terms in square brackets can be practically omitted in either of the two equations and as a first good approximation we obtain

$$\sigma = \int_{P_o}^{P_2}\frac{dP}{\rho} \quad \ldots \quad \ldots \quad \ldots \quad \ldots \quad (10)$$

for both open and closed systems. Defining the mean density from

$$\frac{1}{\rho_m}(P_2 - P_o) = \int_{P_o}^{P_2}\frac{dP}{\rho} \quad \ldots \quad \ldots \quad \ldots \quad (11)$$

and inserting for σ the maximum allowable stress σ_{max} for the blade material due to a certain ω the optimum pressure rise $P_{2max} - P_o$ which can be permitted inside the holes is

$$P_{2max} - P_o = \sigma_{max}(\rho_m/\rho_s). \quad \ldots \quad \ldots \quad (12)$$

This criterion (12) expresses that the maximum radial pressure rise permitted in the cooling passages of any kind of thermosyphon cooling is approximately equal to the mean density ratio of coolant to blade solid times the maximum tensile stress which is permitted for the blade under working conditions and which, of course, fixes the angular velocity ω. Assuming σ_{max} = 14.25 tons/sq.in. = 31900 lb./sq.in. and again ρ_m/ρ_s = 1/10 for water working along the saturation line we obtain $P_{2max} - P_o$ = 3190 lb./sq.in. or, in other words, with P_o = atmospheric pressure is just about equal to the critical pressure of water. On the other hand, σ_{max} = 14.25 tons/sq.in. is just the tensile stress under which 0.1% creep is reached with Nimonic 90 at about 750°C after 300 hours running.

It is thus proved that with the best blade materials it is impossible to exceed 375°C in water as thermosyphon coolant without endangering the blades and as closed thermosyphon cooling as has been shown in a previous chapter is bound to work above this limiting temperature water seems out of question for this cooling method.

For this reason liquids with high boiling points were considered and, amongst these, liquid metals offer good possibilities. The application of liquid sodium in exhaust poppet valves of reciprocating engines and its low density in connection with its high thermal conductivity suggest the use of sodium in the closed thermosyphon process. Though, according to formula (12), the pressure at the blade tip has to be less than the critical pressure of water, the working line in the pressure-volume diagram would be in the region of sufficiently high temperatures.

APPENDIX III

Correlation methods for closed thermocyphon cooling

Thermosyphon cooling in a vertical hollow cylinder of heated length L, cooled length L' above the heating section and diameter ratio d_o/d_i, as schematically shown in Fig. 4, is a free convection problem and, therefore, the heat transfer between wall and thermosyphon fluid must be governed by a relation of the type:

$$Nu_i = f\left(Gr_1, Pr_i, \frac{L}{d_i}, \frac{\Delta T_1}{T_{s_1}}, T_{s_i}, \frac{L'}{d_i}\right) \quad \ldots \quad \ldots \quad \ldots \quad (13)$$

with

$Nu_i = \frac{h_i d_1}{\lambda_i}$ = Nusselt number, $Gr_i = \frac{d_i^3 b \beta_1 \Delta T_i}{\nu_i^2}$ = Grashof number,

$Pr_i = \frac{\nu_1}{a_1} = \frac{\mu_i C_{p_1}}{\lambda_i}$ = Prandtl number,

h_i = true mean heat transfer coefficient, based on the total heated area $\pi d_i L$ and primary actuating temperature difference ΔT_i in the fluid,

T_{s_i} = absolute standard temperature on which all the properties are based as indicated by suffix 1,

λ_i = thermal conductivity, β_i = thermal expansion coefficient, μ_1 = absolute viscosity, ν_i = kinematic viscosity, C_{p_i} = specific heat, a_i = thermal diffusivity of the liquid, all based on T_{s_i},

b = acceleration acting on the liquid.

An exact determination of equation (13) would require the knowledge of all the movements inside the fluid, i.e. complex investigations. Also the engineer is more interested in more obvious parameters. It appeared simplest to replace ΔT_i by $\Delta T = t_o - \theta_m$ where t_o is the outer wall temperature at the lower (hot) end of the tube and θ_m is the arithmetic mean temperature $\theta_m = \frac{1}{2}(\theta_o + \theta_1)$ between inlet temperature θ_o and outlet temperature θ_1 of the "root" coolant, and to relate all the properties to the temperature t_o at the hot end. The choice of this ΔT is convenient for the engineer and that of t_o as standard temperature resulted from plotting the results which then shew the least amount of scattering. In doing so formula (13) must be rewritten as

$$Nu = f_1\left(Gr, Pr, \frac{L}{d_i}, \frac{\Delta T}{T_o}, T_o, \frac{L'}{d_i}, H_o, H_c\right) \quad \ldots \quad \ldots \quad (14)$$

with $T_o = t_o + 273$ in deg.K, H_o and H_c are the heat resistances for heat input and heat extraction from the thermosyphon fluid,

$Nu = \frac{h d_i}{\lambda}$, $Gr = \frac{d_1^3 b \beta \Delta T}{\nu^2}$, $Pr = \frac{\mu C_p}{\lambda}$, all the properties without suffix are now related to t_o, and h is defined from

$$q = h \pi d_i L \Delta T \quad \ldots \quad \ldots \quad \ldots \quad \ldots \quad \ldots \quad (15)$$

with q for heat extraction rate, and therefore

$$Nu = \frac{h d_i}{\lambda} = \frac{q}{\pi L \lambda \Delta T}.$$

In the present investigations the effects of H_o, H_c, T_o and $\frac{\Delta T}{T_o}$ could not be investigated separately and had to be left uncorrelated. The remaining main parameters were correlated in the form

$$Nu = C\ Gr^{m_1}\ Pr^{m_2} \left(\frac{L}{d_1}\right)^{m_3} \left(\frac{L'}{d_i}\right)^{m_4} \quad \ldots \quad \ldots \quad (17)$$

with C and m_2 as universal constants, while m_1 depends on the character of flow, i.e. whether the flow is laminar or turbulent, and m_3 and m_4 may depend on some property of the fluid. Due to the neglect of the other parameters a plot of the tests in the form of (17) will include a certain amount of scattering. Nevertheless the plot will provide ample evidence for the calculation of the heat extracting power of any other thermosyphon fluid, such as liquid sodium in turbine blades. In these calculatins, of course, t_o must be interpreted as the hot end wall temperature t_{o_1} inside the hole (see Fig. 4). This is justified because d_o/d_1 in the tests was only of the order 1.03.

Another possibility of representing the results is based on the conception of apparent conductivities. Assuming a cylindrical solid rod of length L, diameter d_o and thermal conductivity λ_M with uniform heat input q_o per unit time per unit area around the perimeter over length element dx, the temperature distribution t in the rod over length L is determined by

$$\frac{d^2t}{dx^2} = - \frac{4q_o}{d_o \lambda_M}, \quad \ldots \quad \ldots \quad (18)$$

with the simplifying assumption that λ_M is high enough to allow the problem t_o be treated as one-dimensional. Measuring the length from the hot end, having the temperature t_o, and assuming that also $dt/dx = o$ at this end, the integration gives

$$t = t_o - \frac{4}{d_o} \int_o^x \int_o^x \frac{q_o}{\lambda_M}\ dx\ dx \quad . \quad \ldots \quad \ldots \quad (19)$$

If λ_M can be taken as independent of x and q_o is a constant over the whole length L, then

$$t = t_o - \frac{q\,x^2}{2AL\lambda_M} \quad \ldots \quad \ldots \quad (20)$$

with A as cross-sectional area of the rod and $q = \pi d_o L q_o$ = total heat input.

For the case of a solid copper rod equation (20) holds very well near the hot end so that q_o is practically independent of x. This was verified by measuring, in one case, the heat transport through a solid copper element. The parabolic relation does not hold for the liquid filled elements. Assuming, however, as a first approximation its validity for the thermosyphon tubes, the ratio of the apparent conductivity λ_{app} to the conductivity of solid copper $\lambda_{M_{Cu}}$ in the same geometrical arrangement and with the same total heat extraction q is given by

$$\lambda_{app}/\lambda_{M_{Cu}} = \left(t_{o_{C_u}} - t_{C_u}\right) / \left(t_{o_L} - t_L\right),$$

the suffixes C_u and L denoting values in the copper rod and the liquid tube respectively.

APPENDIX IV

List of Symbols

A cross-sectional area of tube, of solid bar, or of solid material of turbine blade

a_i thermometric conductivity of fluid based on reference temperature T_{s_i}

b radial acceleration in turbine blade

C empirical constant

C_p specific heat based on reference temperature t_o

C_{p_g} specific heat of working gas in turbine

C_{p_i} specific heat of fluid based on T_{s_i}

C_{p_w} specific heat of water

d_i inner diameter of tube

d_o outer diameter of tube

G mass flow rate through actual turbine

Gr Grashof number based on t_o

Gr_i Grashof number based on T_{s_i}

g acceleration due to gravity

H_o heat resistance at hot end of thermosyphon tube

H_c heat resistance at cold end of thermosyphon tube

h heat transfer coefficient based on ΔT

h_i heat transfer coefficient based on ΔT_i

j dimensionless heat transfer coefficient, function of Gr only

L heated length of test tube

L' cooled length of test tube

M weight of cooling water in time z

m_s mass of blade material

m_1 mass of fluid in holes

m_1, m_2, m_3, m_4 empirical exponents in power law

Nu Nusselt number based on t_o and h

Nu_i Nusselt number based on T_{s_i} and h_i

n number of turbine blades

P fluid pressure in hollow turbine blade

P_o lowest fluid pressure in hollow blade at radius r_1 or r_4

P_2, P_3 fluid pressure in hollow blade at radius r_2 and density ρ_1, ρ_2 respevtively

P_{2max} optimum fluid pressure connected to σ_{max}

Pr Prandtl number based on t_o

Pr_i Prandtl number based on T_{s_i}

p per cent of total heat flow extracted by internal blade cooling

Q amount of heat transmitted across wall of tube

q rate of heat extraction by thermosyphon cooling

q_o uniform rate of heat inflow into bar

r radial distance in turbine blade

r_i outer radius of hub

r_l radius of gyration for liquid column in blade

r_N radius of gyration for sodium filling

r_s radius of gyration for solid part of blade

r_W radius of gyration for water column in open thermosyphon system

r_1, r_2 inner and outer radii of liquid column in open system

r_4, r_2 inner and outer radii of liquid column in closed system

r_3 inner radius of liquid column in closed system in cold state

T_{s_i} absolute theoretical reference temperature of thermosyphon fluid

t wall temperature of thermosyphon tube at x

t_o, t_1, t_2, t_3, t_4 measured wall temperatures at defined positions along thermosyphon tube, t_o nearest to lower end, t_4 nearest to cooled end

t_{b_o} gas-side turbine blade surface temperature

t_c temperature of coolant in internally cooled blade

$t_c^{\varkappa}$ critical temperature of coolant in blade

t_g working gas temperature in turbine

x distance from lower end of test element

z time indicated by stop watch for mass flow M of cooling water, or number of cooling holes in turbine blade

β expansion coefficient of thermosyphon fluid at reference temperature t_o

β_i expansion coefficient of thermosyphon fluid at reference temperature T_{s_i}

$\Delta T = t_o - \theta_m$ temperature difference used for correlation

ΔT_i theoretical temperature difference for correlation

δ wall thickness

θ_o inlet temperature of cooling water

θ_1 outlet temperature of cooling water

$\theta_m = \frac{1}{2}(\theta_o + \theta_1)$ mean temperature of cooling water

ϑ wall temperature of thermosyphon tube in middle of cooling coil

λ thermal conductivity of thermosyphon fluid based on t_o

λ_i thermal conductivity of thermosyphon fluid based on T_{s_i}

λ_{app} apparent thermal conductivity of fluid filled tube

λ_M thermal conductivity of solid material

λ_{MCu} thermal conductivity of copper

μ viscosity based on t_o

μ_1 viscosity based on T_{s_i}

ν kinematic viscosity based on t_o

ν_i kinematic viscosity based on T_{s_1}

ρ density of coolant

ρ_1, ρ_2 density of thermosyphon liquid in open, closed system respectively of turbine

ρ_m mean density of liquid in internally cooled blade

ρ_s density of blade solid

σ stress exerted on turbine blade

σ_1, σ_2 stress exerted on turbine blade in the case of open, closed thermosyphon system respectively

σ_{max} maximum stress permitted for turbine blade

Σf total cross section of holes in turbine blade

φ angle between blade axis and direction of gravity

ω angular velocity.

TABLE - 1. DESCRIPTION OF TEST SERIES.

TEST TUBE Nº	MATERIAL	INSIDE DIA d_i [INCHES]	OUTSIDE DIA d_o [INCHES]	HEATED LENGTH L [INCHES] (HEATING WIRE CONSTANTAN OF 21 S.W.G)	$\frac{L}{d_i}$	COOLED LENGTH L' [INCHES]	DESCRIPTION OF COOLING ARRANGEMENT (SEE FOOTNOTE)	NUMBER AND POSITION OF WALL THERMOCOUPLES	THERMOSYPHON LIQUID	LENGTH OF LIQUID COLUMN [INCHES]	SYMBOL APPLIED IN ALL GRAPHS
2	MILD STEEL	1·811	1·872	13 WITH 22 TURNS PER INCH.	7·18	4·375	a	4 IN DISTANCES OF 0·5, 6·5, 12·5 AND 15 2 INCHES FROM BOTTOM	WATER	17·4	□
									MERCURY	17 4	■
							b		MERCURY	17·4	▲
2a	MILD STEEL, INSIDE TINNED WITH TINMANS SOLDER TO INDUCE MERCURY WETTING.	1·811	1·872	13 WITH 18 TURNS PER INCH.	7·18	4·375	a	6 IN DISTANCES OF 0·5, 3·5, 6 5, 9·5, 12·5 AND 15·2 INCHES FROM BOTTOM	MERCURY	17·4	✱
4	STAINLESS STEEL	1·805	1·873	13·5 WITH 18 TURNS PER INCH	7·48	4 50	a	6 IN DISTANCES OF 0·5, 3·5, 6·5, 9·5 12·5 AND 15·75 INCHES FROM BOTTOM	MERCURY	18·0	×
									WATER	18·0	+
									TRANSFORMER OIL	18·0	⋎
							c	AS ABOVE.	TRANSFORMER OIL	18·0	⋏
							d	AS ABOVE	TRANSFORMER OIL	18·0	⋗
7	MILD STEEL	1·310	1·373	13 WITH 18 TURNS PER INCH.	9 924	5·0	a	6 IN DISTANCES OF 0·5, 3·5, 6·5, 9·5 12·5 AND 15·5 INCHES FROM BOTTOM.	MERCURY	18·0	▼
									MERCURY	16·1	▼
									WATER	18·0	▽
									TRANSFORMER OIL	18·5	▽
6	SOLID COPPER BAR	0	1·812	13 WITH 18 TURNS PER INCH.	L/d_o = 7·17	4·50	a	6 IN DISTANCES OF 0·5 3·5, 6·5, 9·5, 12·5 & 15·25 INCHES FROM BOTTOM	—	—	⊙

TEST TUBE Nº	MATERIAL	INSIDE DIA d_i [INCHES]	OUTSIDE DIA. d_o [INCHES]	HEATED LENGTH L [INCHES] (HEATING WIRE CONSTANTAN OF 21 S.W.G)	$\frac{L}{d_i}$	COOLED LENGTH L' [INCHES]	DESCRIPTON OF COOLING ARRANGEMENT (SEE FOOTNOTE)	NUMBER AND POSITION OF WALL THERMOCOUPLES	THERMOSYPHON LIQUID	LENGTH OF LIQUID COLUMN [INCHES]	SYMBOL APPLIED IN ALL GRAPHS
3	STAINLESS STEEL	0·925	0 955	13 WITH 20 TURNS PER INCH	14 05	4 50	a	6 IN DISTANCES OF 0·5, 3·5, 6·5, 9·5 12·5 AND 15·25 INCHES FROM BOTTOM	MERCURY	17 5	●
									WATER	17 5	○
5	MILD STEEL INSIDE TINNED WITH TINMANS SOLDER TO INDUCE MERCURY WETTING	0 9295	1·00	13 WITH 18 TURNS PER INCH.	13·99	4·50	a	6 IN DISTANCES OF 0·5, 3·5, 6 5, 9·5 12 5 AND 15·25 INCHES FROM BOTTOM.	WATER	17 5	⊹
									MERCURY	17 5	✦
8	MILD STEEL	1·811	1·872	6·5 WITH 18 TURNS PER INCH	3·59	4·375	c	6 IN DISTANCES OF ¼, 1¾, 3¼, 4¾ 6¼ AND 8·44 INCHES FROM BOTTOM	MERCURY	10 9	◖
									WATER	10 9	◐
									TRANSFORMER OIL	10·9	◐
							a	AS ABOVE.	MERCURY	10 9	◗
									WATER	10·9	◑
									TRANSFORMER OIL	10·9	◑
							d	AS ABOVE	MERCURY	10 9	◓
9	MILD STEEL	0 944	0 987	5 69 WITH 18 TURNS PER INCH	6·03	2·75	a	4 IN DISTANCES OF ¼, $2\frac{27}{32}$, $5\frac{7}{16}$ AND $5\frac{11}{16}$ INCHES FROM BOTTOM.	TRANSFORMER OIL	8 5	▲
									WATER	8·5	△
									MERCURY	8 5	▲

TEST TUBE Nº	MATERIAL	INSIDE DIA d_i [INCHES]	OUTSIDE DIA d_o [INCHES]	HEATED LENGTH L [INCHES] (HEATING WIRE CONSTANTAN OF 21 S.W.G.)	$\frac{L}{d_i}$	COOLED LENGTH L' [INCHES]	DESCRIPTION OF COOLING ARRANGEMENT (SEE FOOTNOTE)	NUMBER AND POSITION OF WALL THERMOCOUPLES	THERMOSYPHON LIQUID	LENGTH OF LIQUID COLUMN [INCHES]	SYMBOL APPLIED IN ALL GRAPHS.
10	MILD STEEL, INSIDE COPPER PLATED AND BRAZED TO INDUCE MERCURY WETTING	1·806	1·869	12·5 WITH 18 TURNS PER INCH	6·92	5	a	6 IN DISTANCES OF 0·5, 3⅜, 6¼, 9⅛, 12 AND 15 INCHES FROM BOTTOM.	MERCURY	17·5	○
									TRANSFORMER OIL	17·5	◎
									WATER	17·5	⊕

FOOTNOTE:-

IN COOLING ARRANGEMENT "a" 10 TURNS OF ⅜" O D COPPER PIPE WERE TIGHTLY WOUND ROUND THE UPPER (OPEN) END OF THE TEST TUBE, AND THE SPACES BETWEEN FILLED WITH TINMANS' SOLDER TO FORM A SOLID CONDUCTING BLOCK OF ABOUT 1" THICKNESS. THE COOLING WATER WAS ARRANGED IN "COUNTER" FLOW, i.e ENTERING ON TOP OF THE COOLING COIL AND LEAVING AT LOWER END.

COOLING ARRANGEMENT "b" WAS THE SAME AS "a" BUT WITH COOLING WATER IN "PARALLEL" FLOW, i.e. ENTERING THE COIL AT LOWER END AND LEAVING IT AT UPPER END.

IN COOLING ARRANGEMENT "c" A 22 TURN COIL WITH ¾" O D AND MADE OF ⅜" O.D. 24 S W G STEEL TUBE, THE COIL BEING 4½" LONG, WAS INSERTED INTO CENTRE OF TEST TUBE.

IN ARRANGEMENT "d" BOTH SYSTEMS "a" AND "c" WERE WORKING TOGETHER.

FIG.1.

ELEMENT OF A THERMOSYPHON TUBE.

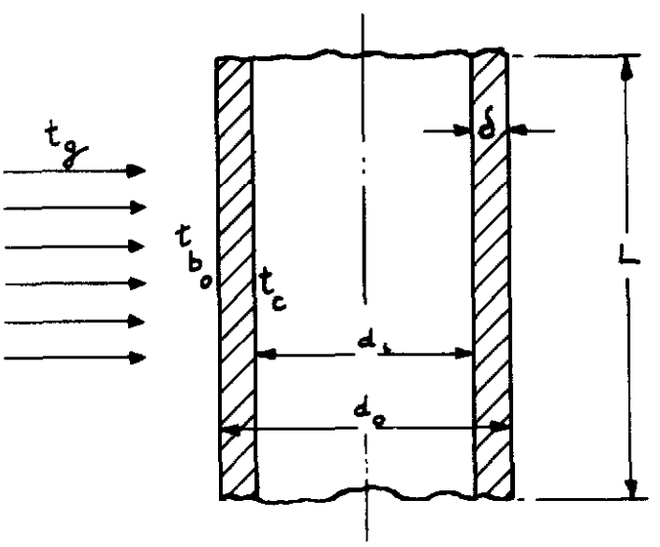

FIG.2.

DIAMETER RATIO d_o/d_i OF HOLES IN OPEN THERMOSYPHON SYSTEM AS FUNCTION OF MASS FLOW THROUGH TURBINE AND AMOUNT OF HEAT EXTRACTION

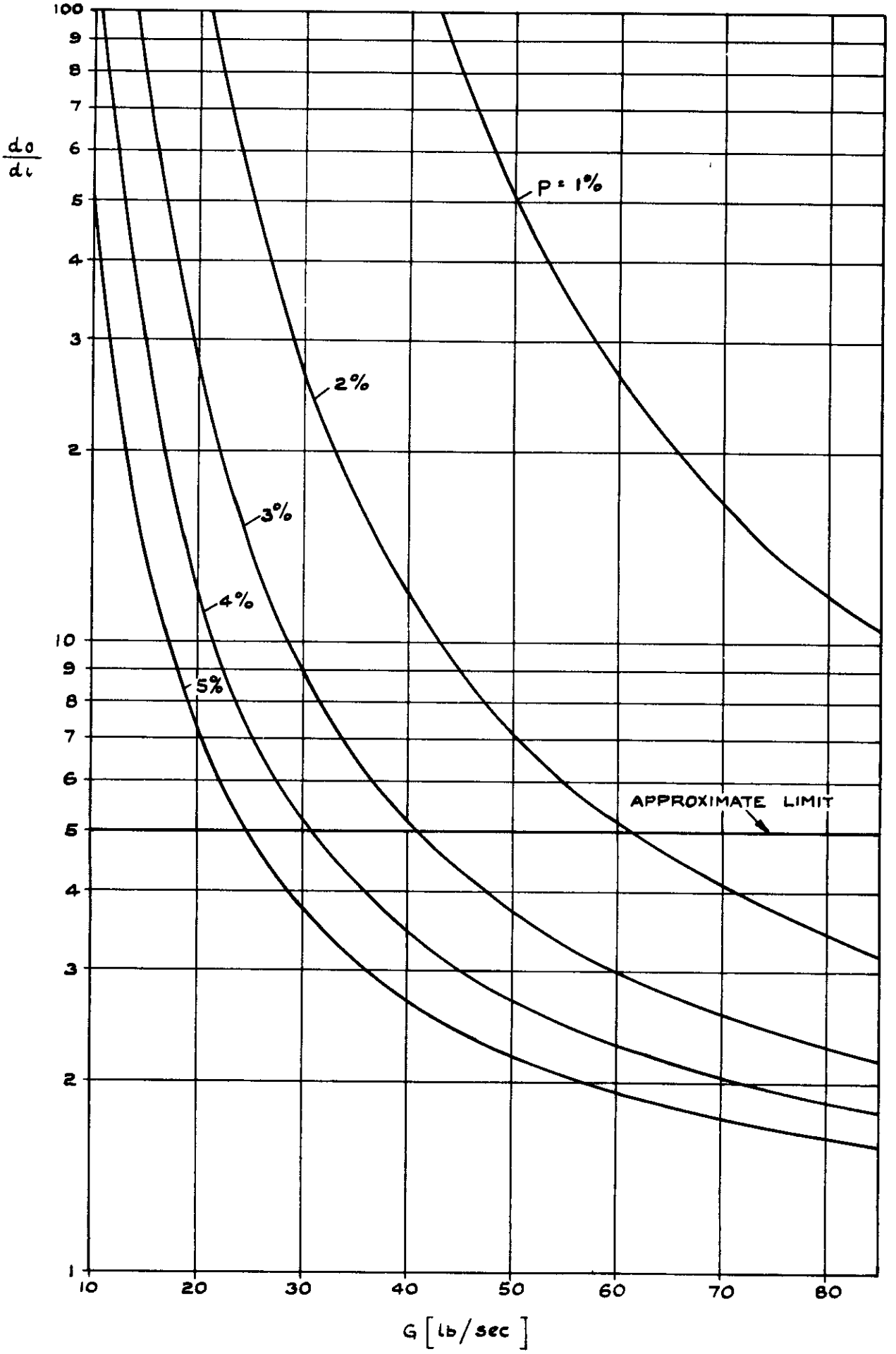

FIG.3.

COMPARISON BETWEEN OPEN AND CLOSED THERMOSYPHON BLADE COOLING (SCHEMATICALLY ONLY)

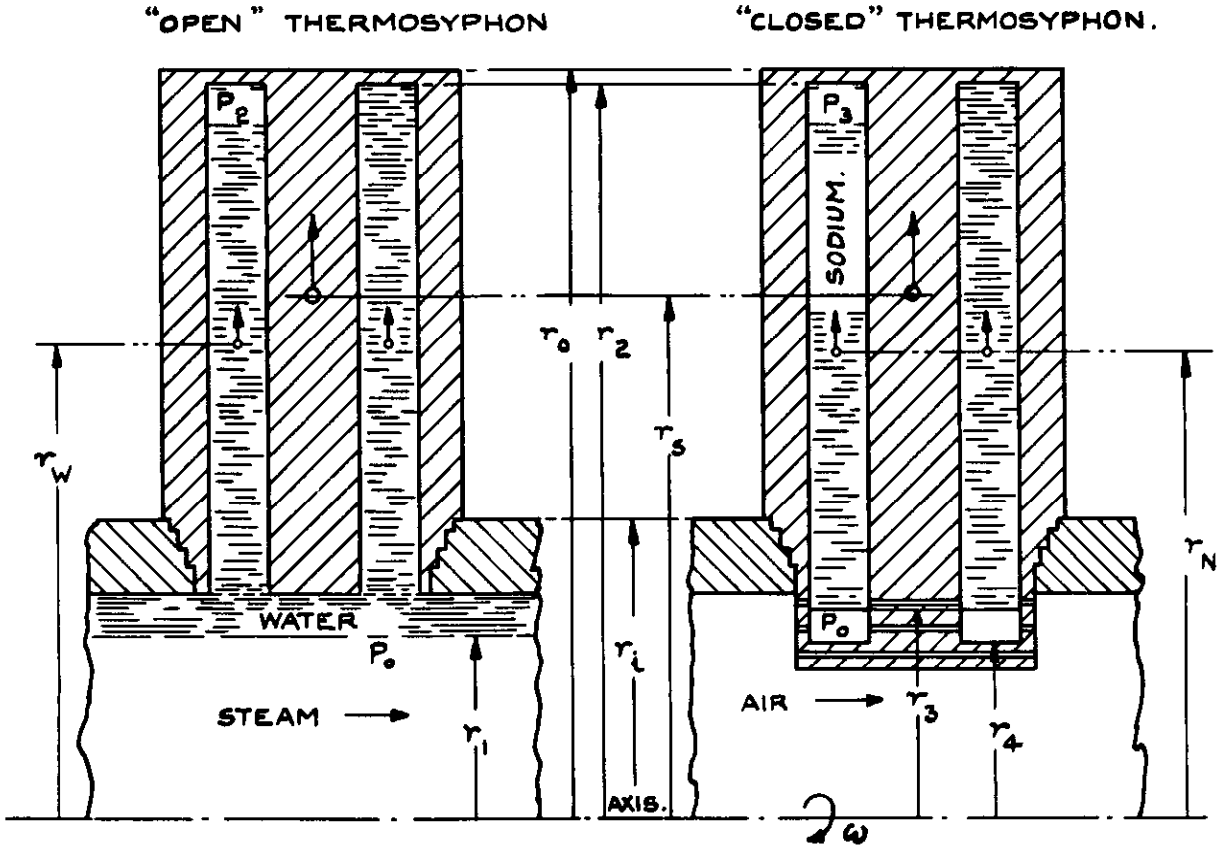

FIG.4.

SCHEME OF TEST ARRANGEMENT

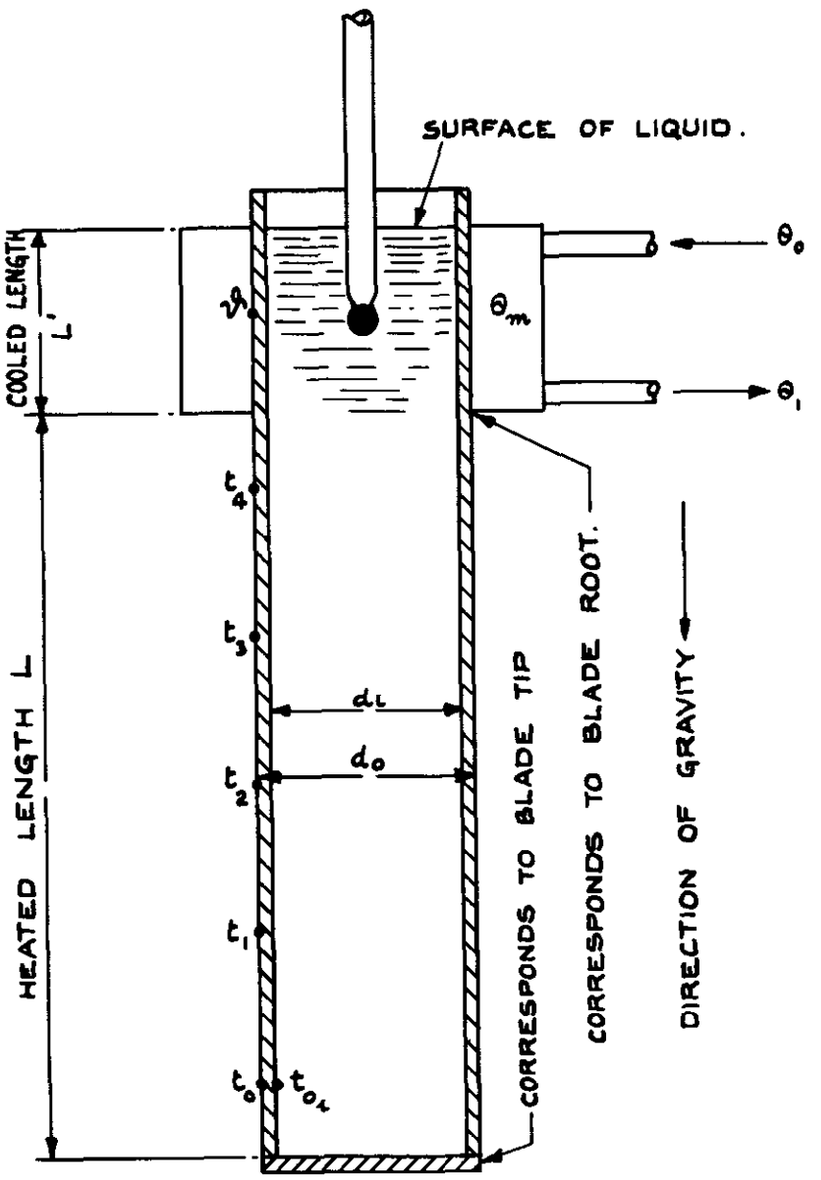

FIG 5.

TEMPERATURE DISTRIBUTION ALONG TEST TUBE Nº 4
WITH MERCURY FILLING (TEST CONDITIONS SEE TABLE 1)

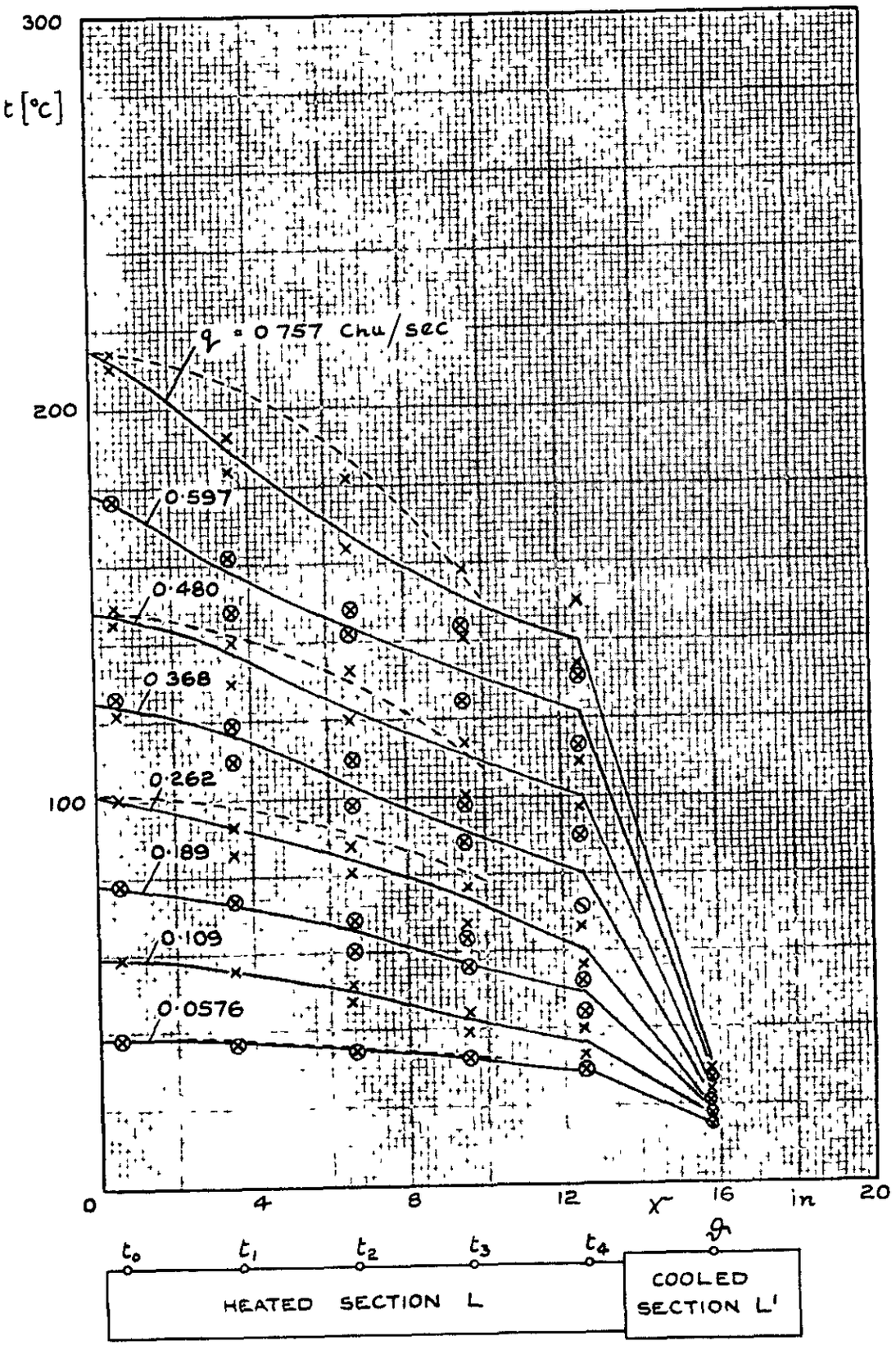

FIG.6.

TEMPERATURE DISTRIBUTION ALONG TEST TUBE Nº 5
WITH WATER FILLING (TEST CONDITIONS SEE TABLE 1.)

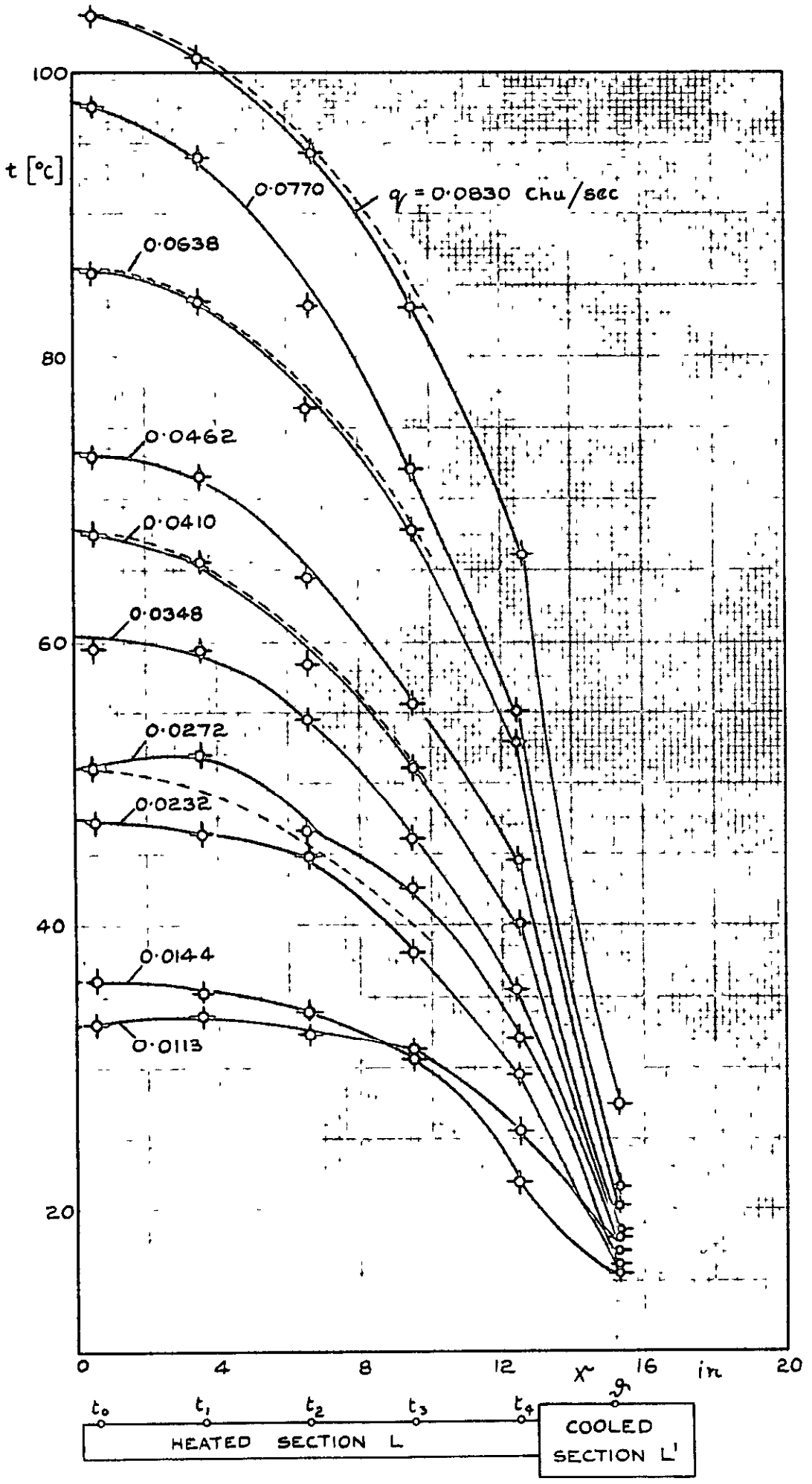

FIG.7.

TEMPERATURE DISTRIBUTION ALONG TEST TUBE № 4
WITH TRANSFORMER OIL FILLING
(TEST CONDITIONS SEE TABLE 1)

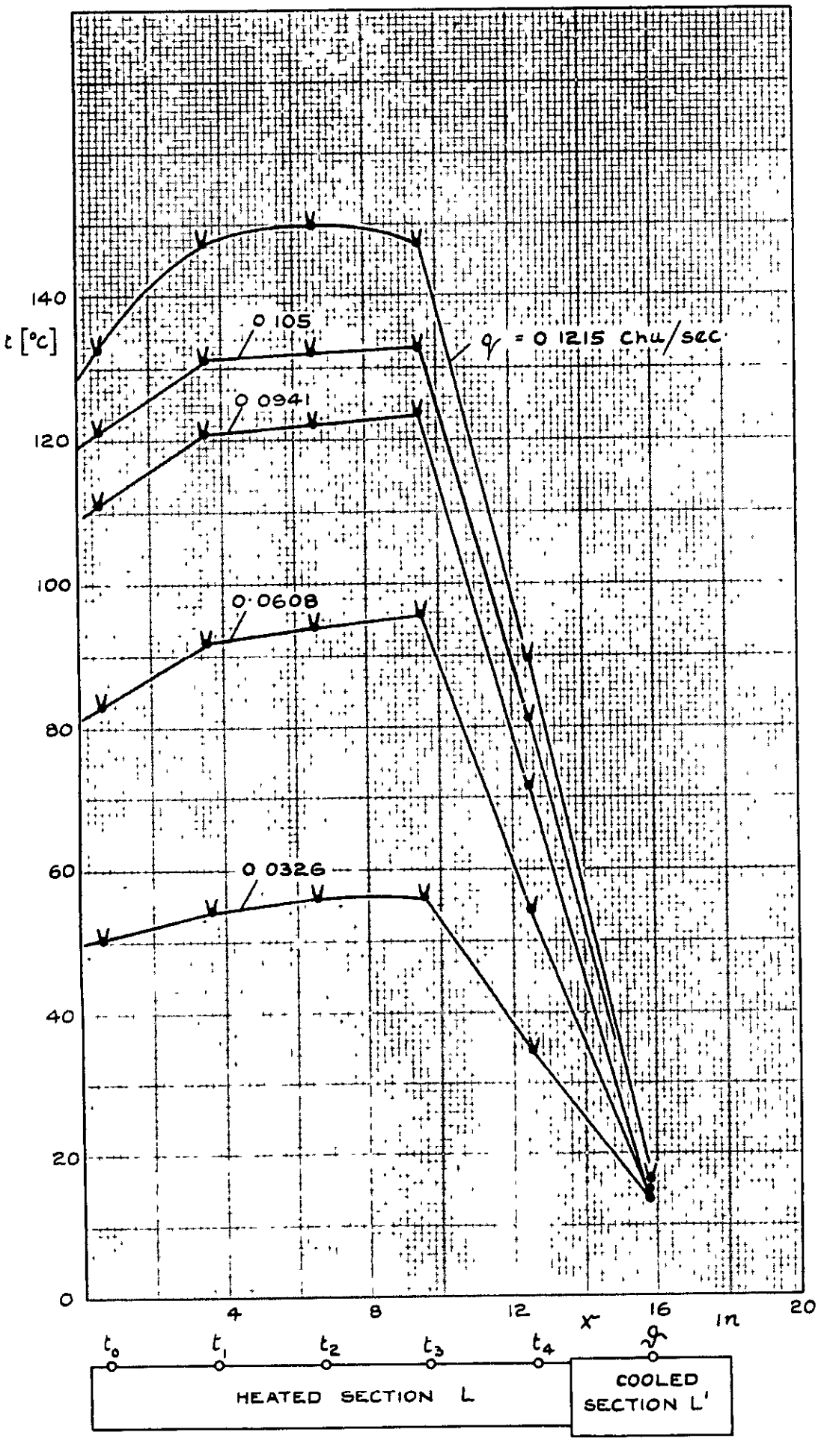

FIG. 8.

TEMPERATURE DISTRIBUTION ALONG SOLID COPPER BAR Nº6.

(SEE TABLE I)

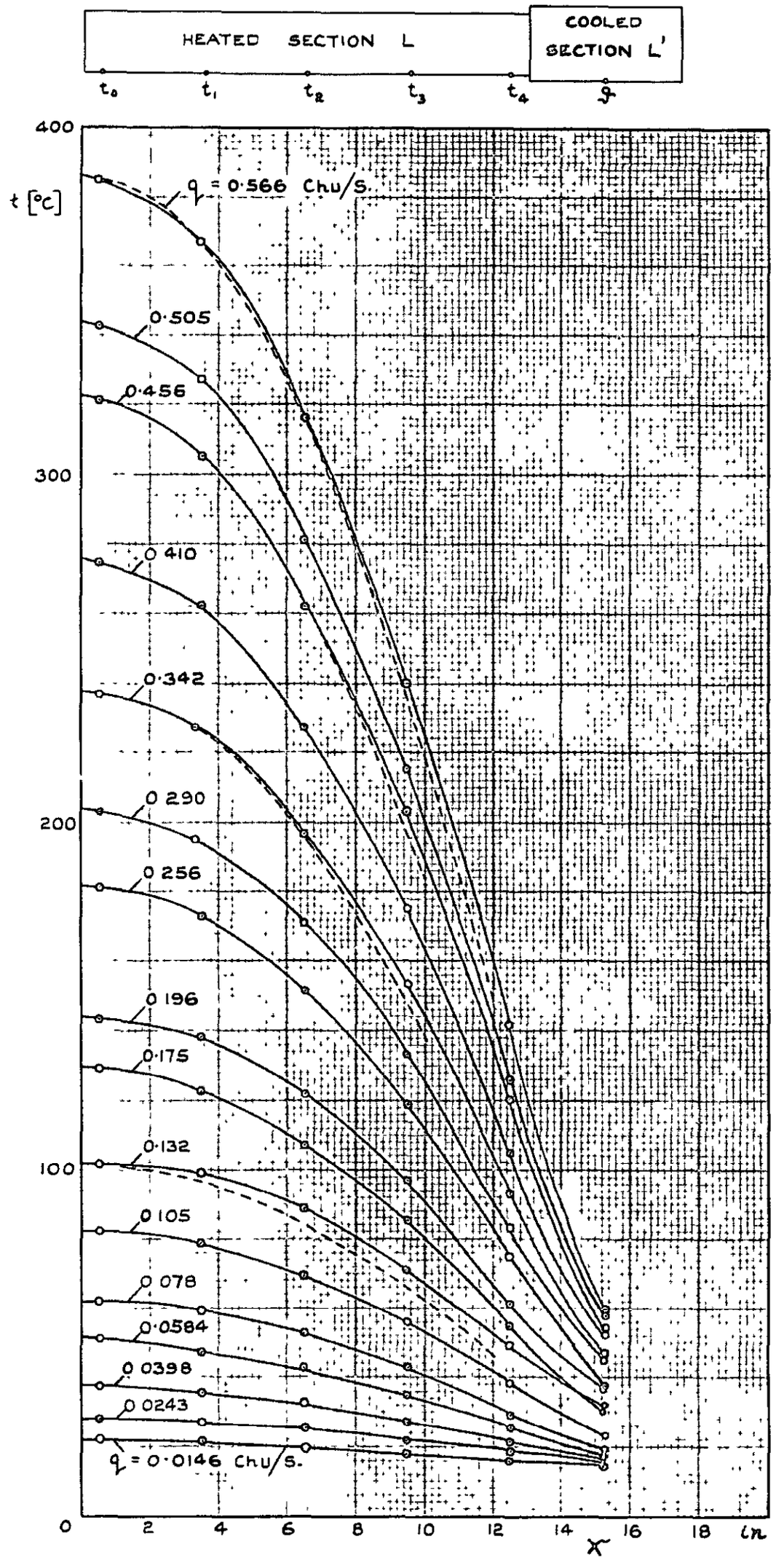

FIG. 9.

RATIO OF APPARENT THERMAL CONDUCTIVITIES OF THERMOSYPHON LIQUID TO THAT OF COPPER FOR THREE LENGTH - DIAMETER RATIOS.

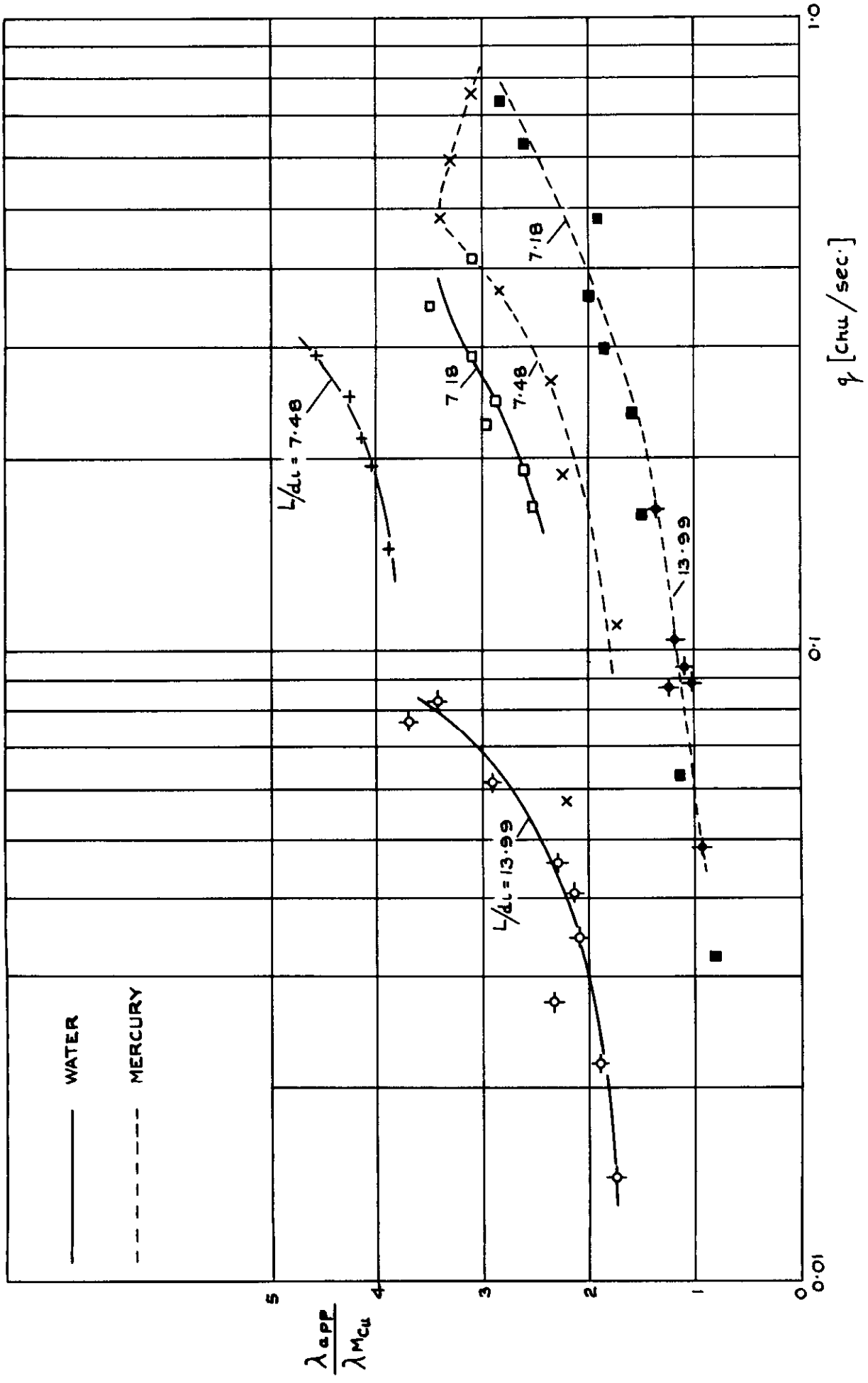

FIG.10a

AMOUNT OF HEAT EXTRACTION q AT TEMPERATURE DIFFERENCE ΔT BETWEEN HOT END OF TUBE AND COOLING WATER WITH COOLING ARRANGEMENT "a" AND "b". (FOR PARAMETERS OF THE CURVES COMPARE WITH SYMBOLS IN TABLE 1.)

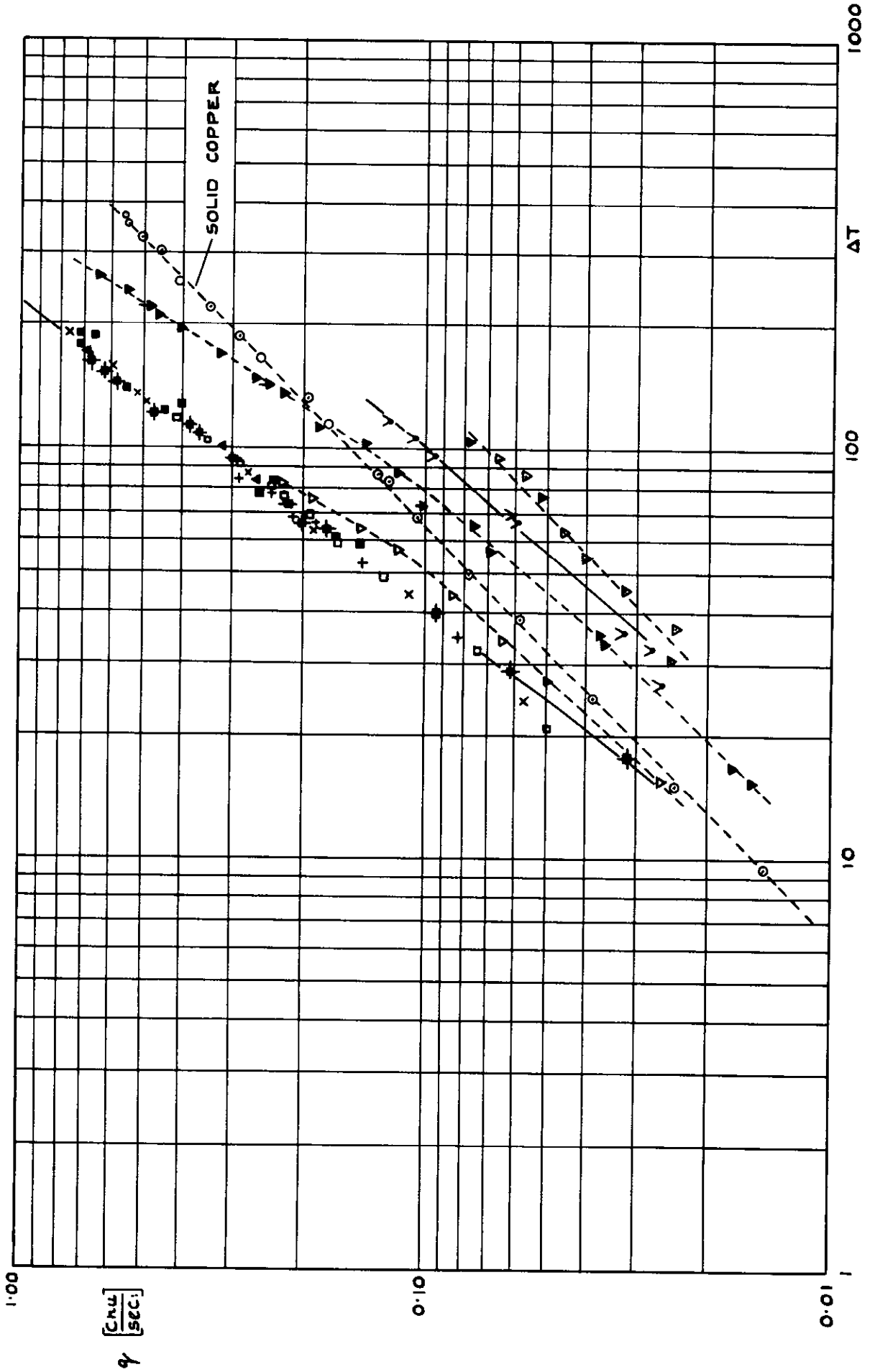

FIG.10,b.

CONTINUATION OF FIG. 10.a

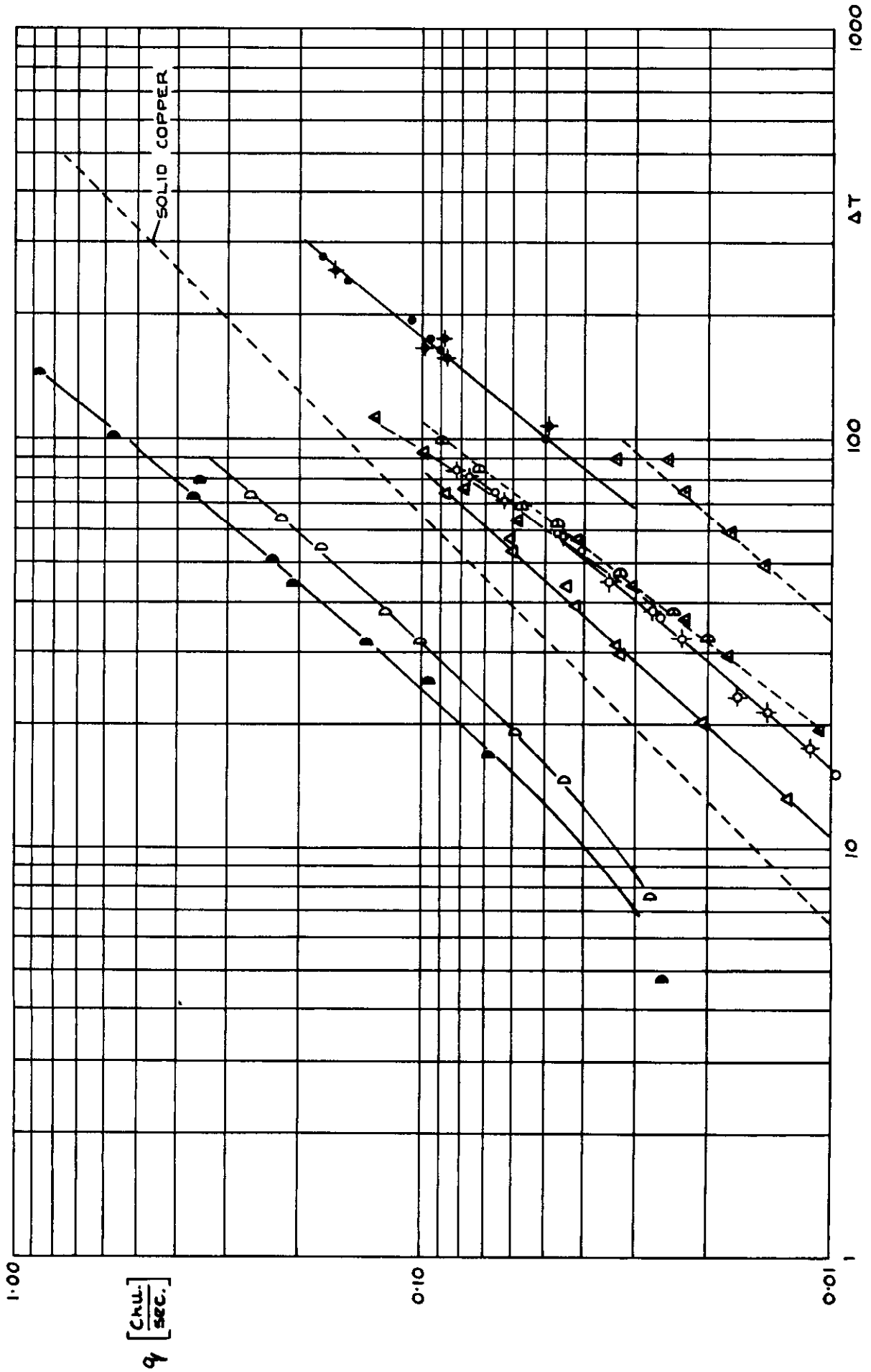

FIG.10.c.

HEAT EXTRACTION q VERSUS TEMPERATURE DIFFERENCE ΔT FOR SOLID COPPER BAR, TUBE 10 WITH COOLING ARRANGEMENT "a", TUBES WITH COOLING ARRANGEMENTS c, d, e, AND TEST TUBE 2 WITH INSERT AND COOLING ARRANGEMENT "a" (FOR PARAMETERS OF THE CURVES COMPARE WITH SYMBOLS IN TABLE 1)

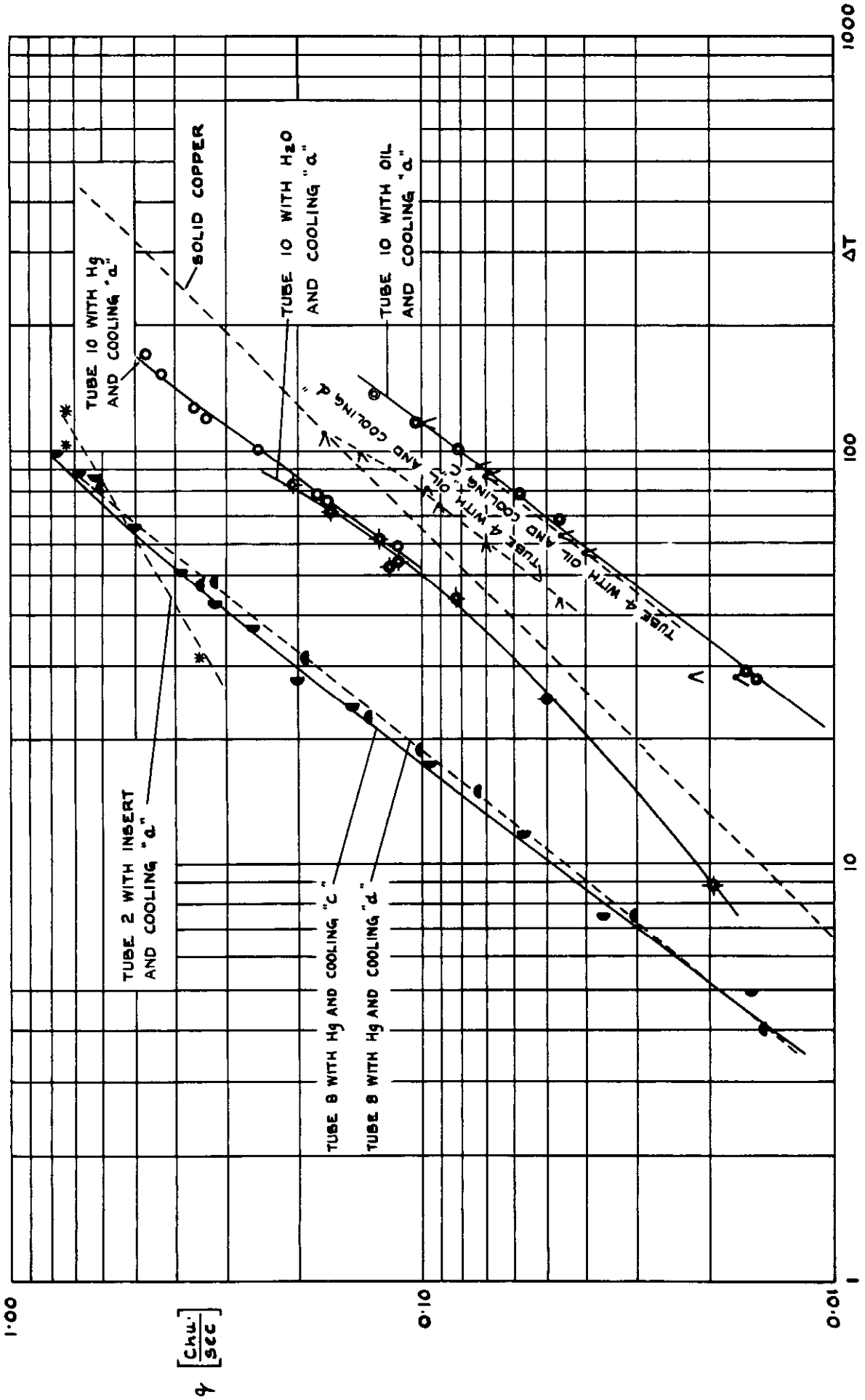

FIG.11.

DIMENSIONLESS HEAT TRANSFER PARAMETER $Nu/Pr^{2/3}$ AS A FUNCTION OF GRASHOF NUMBER Gr FOR ALL TUBES WITH COOLING ARRANGEMENT "a"
NUSSELT NUMBER BASED ON TUBE DIAMETER, TEMPERATURE DIFFERENCE TAKEN BETWEEN HOT END AND MEAN COOLANT, ALL PROPERTIES RELATED TO HOT END

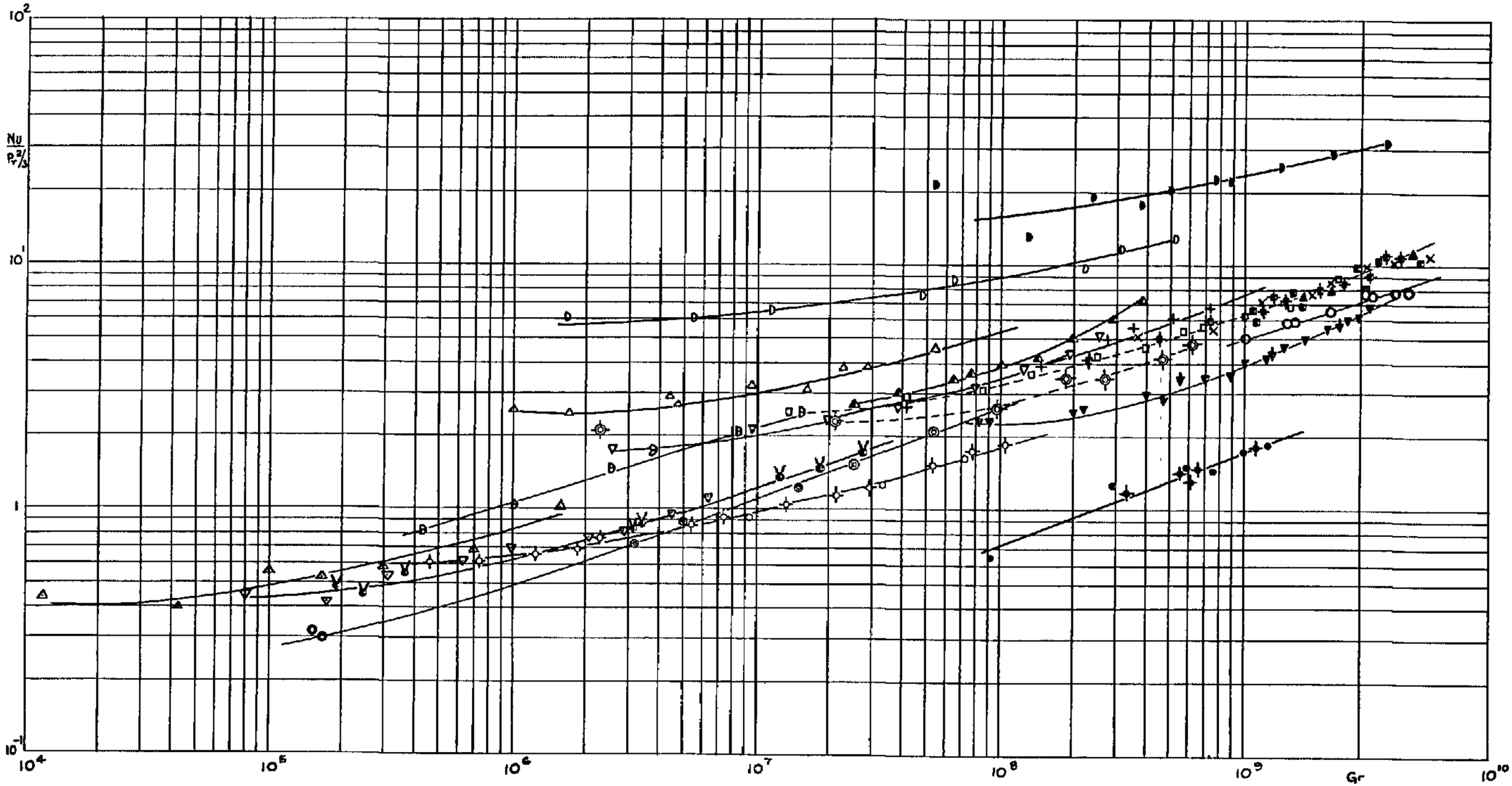

FIG.12.

PROPERTIES OF MERCURY

(FROM LIQUID-METALS HANDBOOK; REF [7])

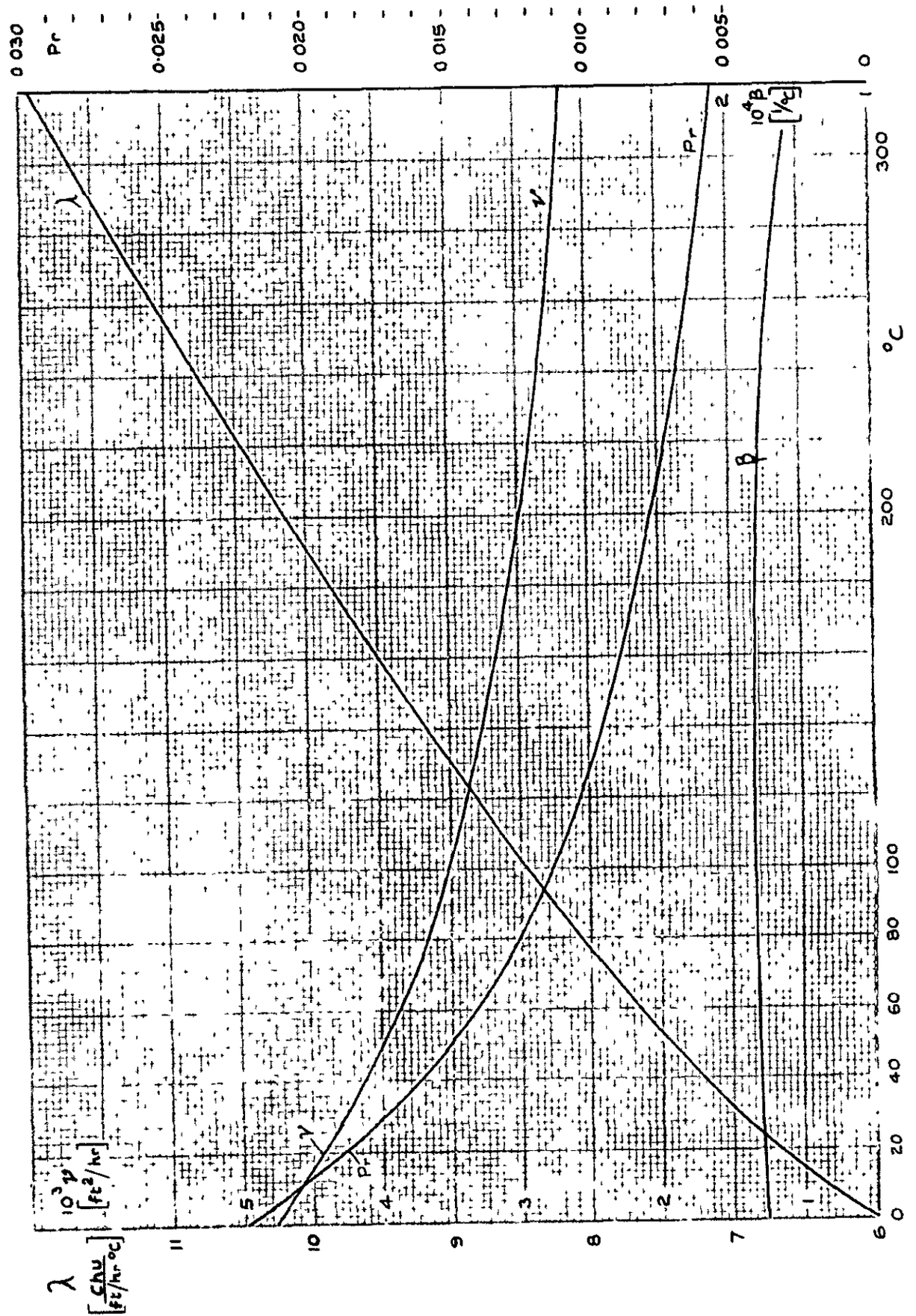

FIG.13.

PROPERTIES OF WATER

(FROM E. SCHMIDT, REF: [8])

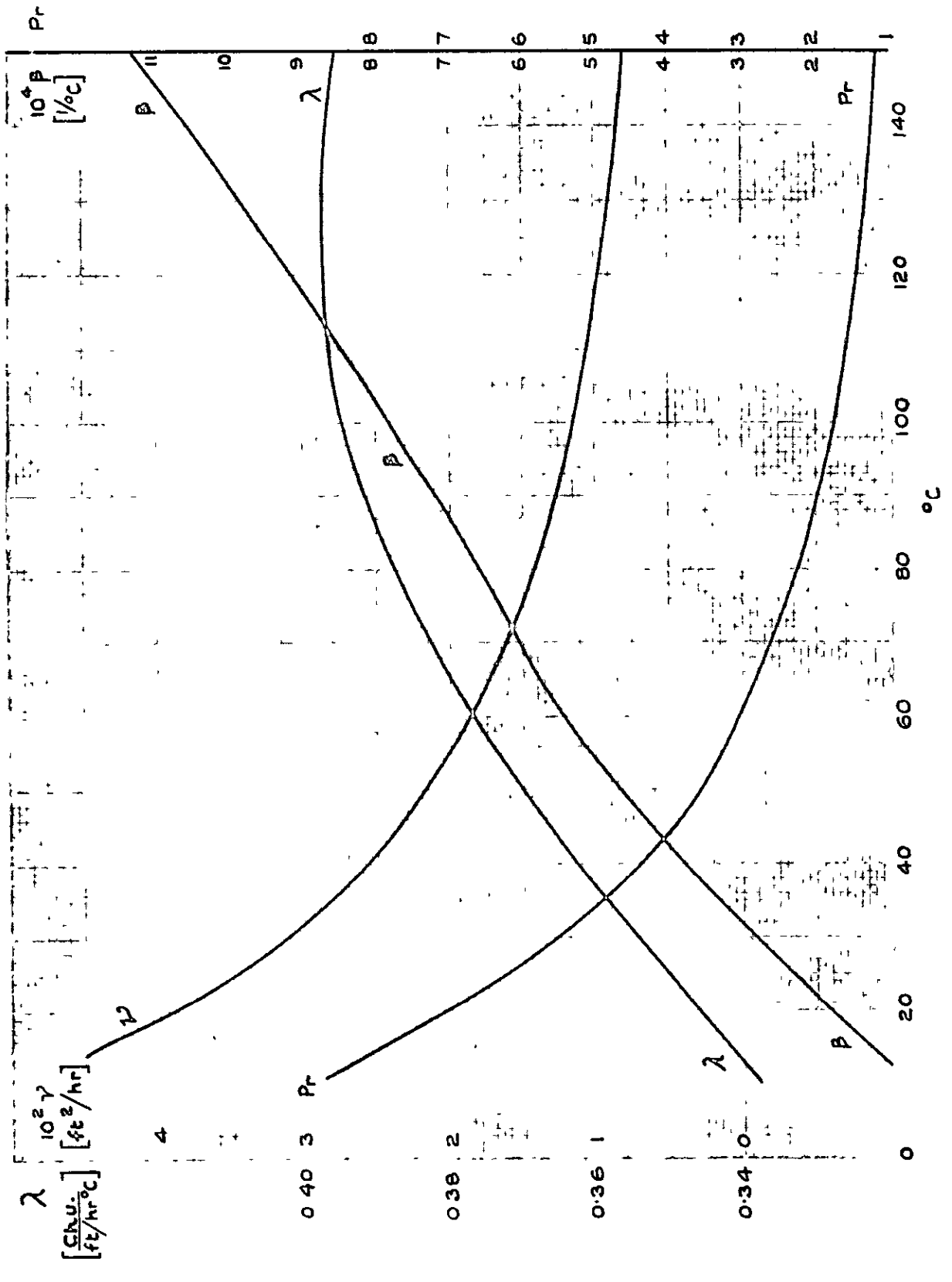

FIG. 14.

PROPERTIES OF TRANSFORMER OIL B.S S.148

AS SUPPLIED BY MANCHESTER OIL REFINERY LTD

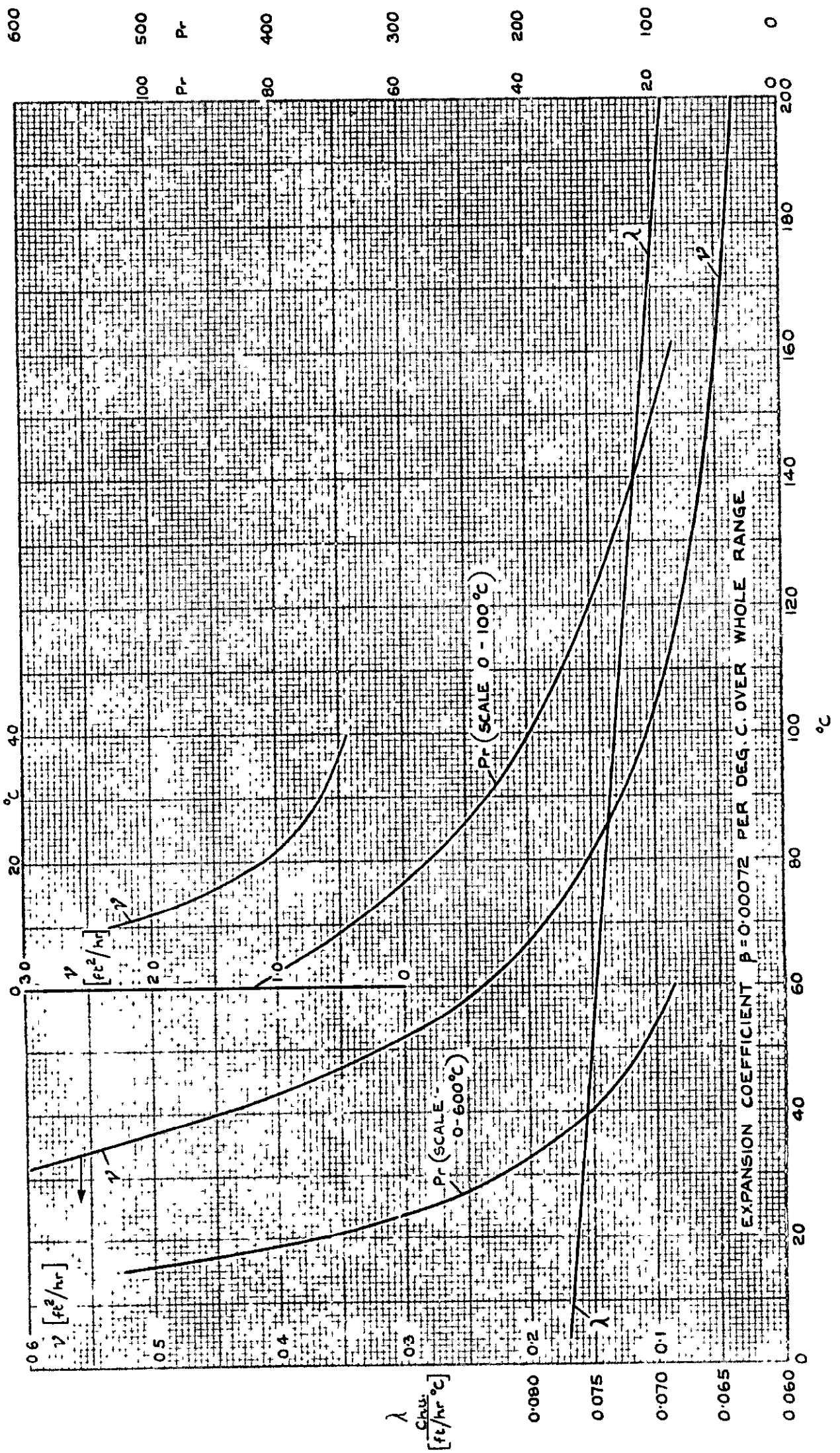

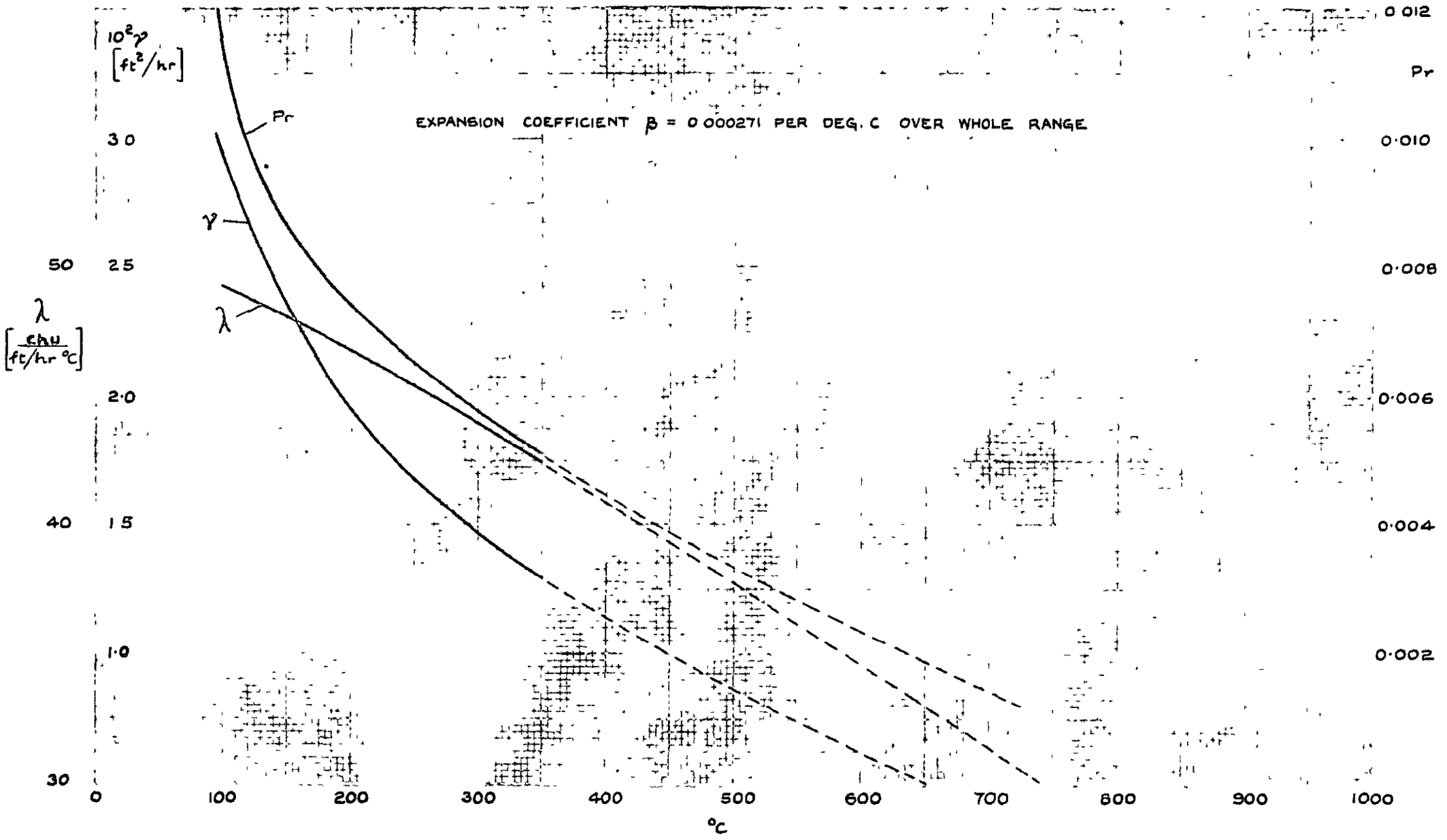
EXPANSION COEFFICIENT β = 0 000271 PER DEG. C OVER WHOLE RANGE
$10^2\gamma$ [ft²/hr]
Pr
γ
λ
λ [chu / ft/hr °C]
Pr
°C
0
100
200
300
400
500
600
700
800
900
1000
30
40
50
1·0
1·5
2·0
2·5
3 0
0 012
0·010
0·008
0·006
0·004
0·002

FIG.15.

FIG.16.

FINAL CORRELATION FOR THERMOSYPHON TUBES

$$\gamma = \frac{Nu}{Pr^{2/3}} \frac{\left(0.1392 \frac{L}{D}\right)^{1.85\left(1 - 0.0979\, Pr^{0.4035}\right)}}{\left(0.415 \frac{L'}{D}\right)^{2.1\left(1.05\, Pr^{0.01} - 1\right)}} = 0.0028373\, Gr^{0.372}$$

γ

10^2

10

1

10^{-1}

10^5 10^6 10^7 10^8 10^9 10^{10} 10^{11}

Gr

FIG 17.

THERMOSYPHON EFFECT OF LIQUID SODIUM IN GAS TURBINE BLADES

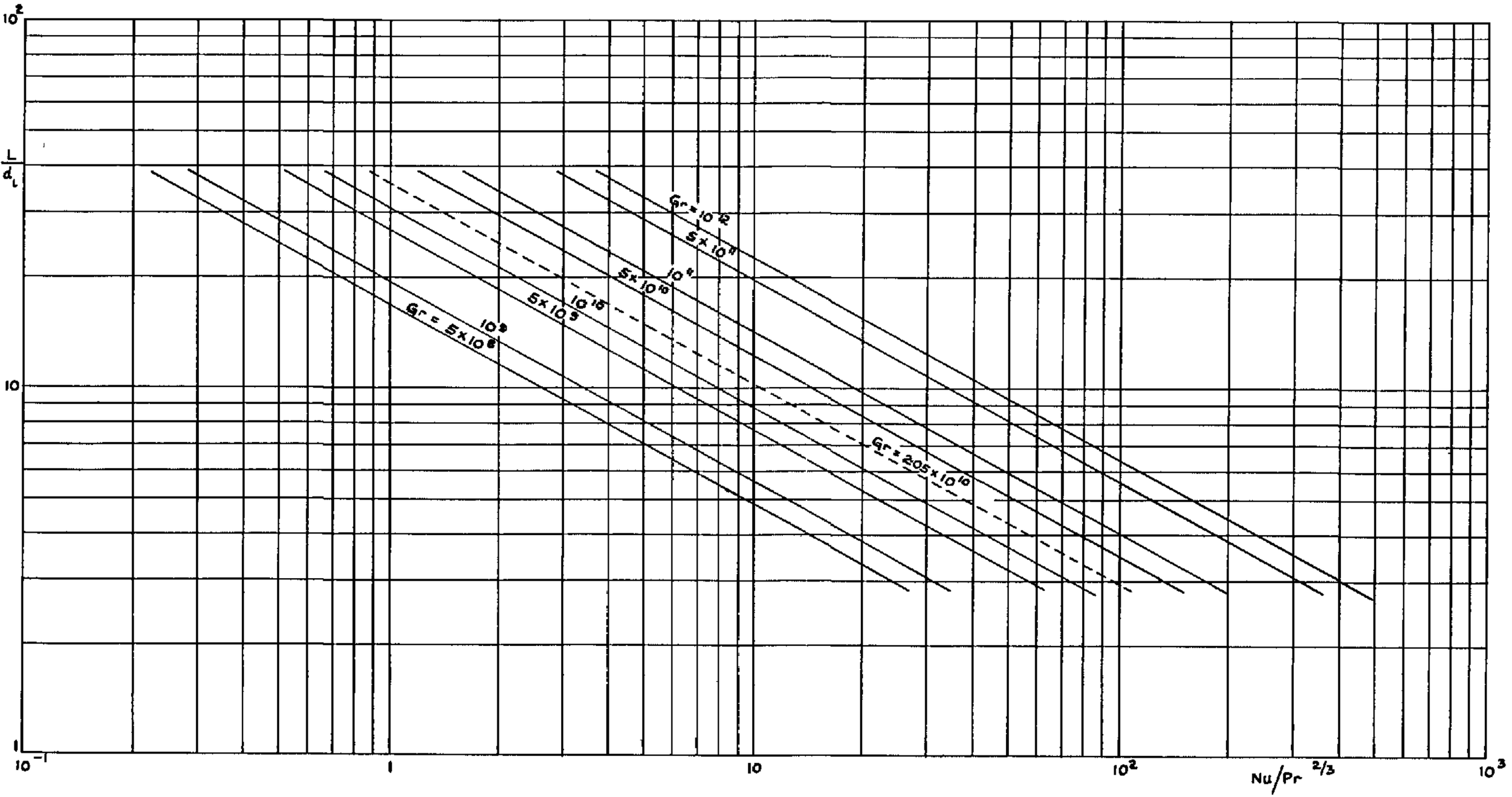

FIG.18.

HEAT EXTRACTION FROM TURBINE BLADES BY LIQUID SODIUM.

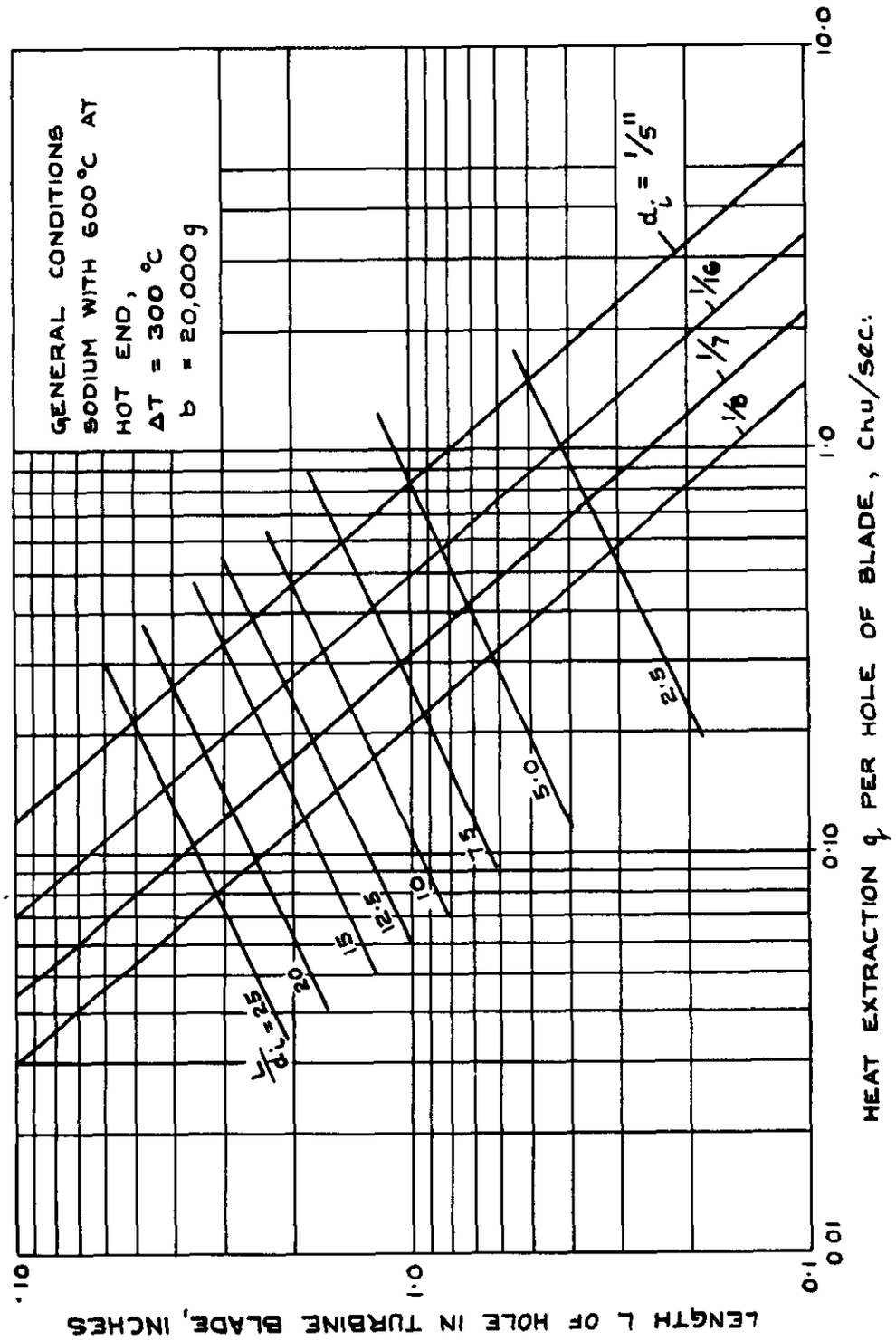

CP No 152
(14,672)
A R.C Technical Report

PRINTED AND PUBLISHED BY HER MAJESTY'S STATIONERY OFFICE
To be purchased from
York House, Kingsway, LONDON, W.C.2 423 Oxford Street, LONDON, W.1
P O. Box 569, LONDON, S E.1
13a Castle Street, EDINBURGH, 2 1 St. Andrew's Crescent, CARDIFF
39 King Street, MANCHESTER, 2 Tower Lane, BRISTOL, 1
2 Edmund Street, BIRMINGHAM, 3 80 Chichester Street, BELFAST
or from any Bookseller
1954
Price 3s 6d net
PRINTED IN GREAT BRITAIN

S O Code No. 23-9007-52